

Causal Imitation Learning Under Measurement Error and Distribution Shift

Shi Bo and AmirEmad Ghassami
 Department of Mathematics and Statistics, Boston University

Abstract

We study offline imitation learning (IL) when part of the decision-relevant state is observed only through noisy measurements and the distribution may change between training and deployment. Such settings induce spurious state–action correlations, so standard behavioral cloning (BC)—whether conditioning on raw measurements or ignoring them—can converge to systematically biased policies under distribution shift. We propose a general framework for IL under measurement error, inspired by explicitly modeling the causal relationships among the variables, yielding a target that retains a causal interpretation and is robust to distribution shift. Building on ideas from proximal causal inference, we introduce **CausIL**, which treats noisy state observations as proxy variables, and we provide identification conditions under which the target policy is recoverable from demonstrations without rewards or interactive expert queries. We develop estimators for both discrete and continuous state spaces; for continuous settings, we use an adversarial procedure over RKHS function classes to learn the required parameters. We evaluate **CausIL** on semi-simulated longitudinal data from the PhysioNet/Computing in Cardiology Challenge 2019 cohort and demonstrate improved robustness to distribution shift compared to BC baselines.

Keywords— Imitation Learning; Measurement Error; Distribution Shift; Causal Inference; Spurious Correlation

1 Introduction

Imitation learning (IL) aims to learn a decision policy from expert demonstrations, without requiring an explicit reward specification. The simplest and most widely used approach is *behavioral cloning* (BC), which reduces IL to supervised learning by fitting a policy that predicts the expert’s action from the agent’s observation (Pomerleau, 1989). Beyond BC, inverse reinforcement learning (Ng and Russell, 2000) and generative adversarial imitation learning (Ho and Ermon, 2016a) is proposed. An important challenge in many real-world settings is that the true state driving the dynamics and expert decisions is *not directly observed*, and the learner instead receives *measurements corrupted by error*. These errors can include noise or systematic sensor bias. For example, in clinical decision making, clinicians act based on latent aspects of patient condition (e.g., disease severity, overall physiological stability) that may not be directly recorded, while a learning system observes noisy proxies such as vital signs and lab values that can be affected by device calibration, charting practices, or protocol differences across hospitals. Analogously, in robotics and autonomous driving, the physical quantities relevant for decision making (e.g., object pose, road friction, occluded agents) are only available through imperfect sensors and perception pipelines whose errors may drift over time.

In this setting, a natural baseline is still to run BC on the available measurements: treat the measurement vector as the policy input and learn $\pi(a | o)$ by supervised regression. This is often a sensible choice when

| Paper | Temporal Confounding | Approach | Delayed Effect | Off-Policy |
|----------------------|----------------------|----------------------------------|--|------------|
| Zhang et al. (2020) | ✗ | Backdoor / Frontdoor Adjustment | None | Yes |
| Kumor et al. (2021) | ✗ | Backdoor Adjustment (Sequential) | None | Yes |
| Swamy et al. (2022a) | ✗ | Instrumental Variable | $U_{t-1} \rightarrow A_t$ | Yes |
| Swamy et al. (2022b) | ✗ | Bayesian + Moment Matching | None | No |
| Zeng et al. (2025) | ✓ | Instrumental Variable | $U_{t-k} \rightarrow A_t$ | Yes |
| Shao et al. (2025) | ✓ | Instrumental Variable | $U_{t-1} \rightarrow S_t$ | Yes |
| Ours | ✓ | Proxy-Based Causal Inference | $A_{t-1} \rightarrow U_t, U_{t-1} \rightarrow A_t$ | Yes |

Table 1: Comparison of causal imitation learning frameworks with unobserved confounders. **Temporal Confounding** indicates whether the method explicitly models hidden variables that evolve over time. **Delayed Effect** lists whether past variables influence future actions.

there is *no distribution shift*—that is, when the joint distribution of the latent state and the measurement process remains stable between training and deployment. Under such stability, the learned mapping from measurements to expert actions can generalize in the usual supervised-learning sense, and including the measurements (rather than discarding them) is typically beneficial because they carry information about the latent state. Distribution shift can be due to the environment and/or sensing pipeline changes across domains. This arises, for instance, when a policy trained in one hospital is deployed in another with different device calibration or measurement protocols, or when a driving policy trained with one camera stack is deployed with different calibration or weather-induced perception errors. Under shift, purely observational feature-action correlations can become unreliable; in particular, BC can latch onto spurious predictors that are not causally stable across domains, and more information can even hurt due to causal misidentification (de Haan et al., 2019). Related causal formulations study imitation when the learner and expert have mismatched sensory inputs and unobserved variables affect decisions (Zhang et al., 2020; Kumor et al., 2021).

This paper focuses on the regime where *measurement error and distribution shift coexist*. We demonstrate that in this regime, standard BC can suffer *systematic bias*—bias that does not disappear even as the trajectory length grows and the amount of demonstration data increases. Moreover, this pathology is not avoided by simple design choices: both (i) BC that conditions on the raw measurements and (ii) BC variants that exclude measurements or rely on naive denoising can converge to biased targets under shift, because the learned associations depend on non-invariant measurement mechanisms and shifted visitation distributions. Motivated by this, we propose an alternative target policy that one should prefer over the standard BC target. Our proposal is inspired by explicitly modeling the *causal relationships* among latent state, measurements, and actions. Rather than imitating the observational conditional $p(a | o)$, we define an *optimal causal imitation policy* that is constructed to be robust to changes in (a) the distribution of latent states and (b) the measurement process by reasoning about how actions affect future variables under intervention.

A key difficulty is that this causal-optimal policy is not always identified from observational demonstrations alone. We provide identification results that characterize when it *is* identifiable and derive estimands based on measurement variables, drawing inspiration from the proximal causal inference framework for unobserved confounding (Miao et al., 2018; Tchetgen Tchetgen et al., 2020). We then develop estimation strategies for the optimal policy in both discrete and continuous settings. For discrete state/measurement spaces, we give an estimator based on solving sample analogues of the identification moment equations. For continuous settings, we propose an adversarial estimation approach over RKHS function classes.

1.1 Related Work

Imitation learning. Behavioral cloning casts imitation as supervised learning from observations to actions (Pomerleau, 1989). Beyond BC, *inverse reinforcement learning* infers a reward/cost function consistent with demonstrations and then plans under that reward (Ng and Russell, 2000), while occupancy-measure matching approaches such as generative adversarial imitation learning align expert and learner behavior by matching visitation distributions via adversarial training (Ho and Ermon, 2016a). As mentioned earlier, a recurring difficulty across IL methods is distribution shift. We note that distribution shift can arise from (i)

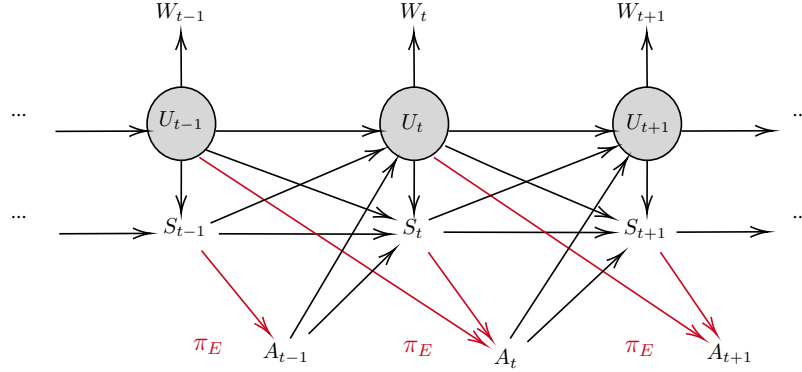


Figure 1: Causal graph for imitation learning under measurement error.

endogenous shift, where the learner’s actions change which states are visited relative to the expert, or (ii) *exogenous* shift, where the environment and/or the sensing (measurement) pipeline changes across domains. The former is the classical IL setting in which compounding errors lead the learner to visit states that are rare or absent in the expert data, motivating interactive data aggregation methods such as DAgger (Ross et al., 2011). In this work, our primary focus is the latter—shifts in the latent state distribution and/or measurement process across domains—and we show that, when combined with measurement error, standard BC can exhibit systematic bias that does not vanish with increasing trajectory length.

Off-policy evaluation under partial observability. A related line of work studies off-policy evaluation (and related identification problems) in partially observed sequential decision processes, including POMDPs with latent confounders, where values/policy performance must be estimated from logged trajectories. Recent approaches introduce estimators to identify and estimate values under latent confounding and partial observability (Tennenholtz et al., 2020; Shi et al., 2022; Miao et al., 2022; Shi et al., 2024; Hong et al., 2024), and proximal reinforcement learning develops efficient off-policy evaluation methods using proxy-variable ideas in partially observed MDPs (Bennett and Kallus, 2024a). These works focus on value estimation with reward feedback, whereas we study imitation without an explicit reward and target a causal-optimal policy under measurement error and distribution shift.

Causal Imitation Learning with Latent Confounding. Recent work has increasingly framed imitation learning as a causal inference problem. Several studies highlight *causal delusion* and related biases in sequential models, where past actions spuriously influence posterior beliefs (De Haan et al., 2019; Ortega et al., 2021). Interactive deconfounded IL methods correct this bias by treating actions as interventions and rely on on-policy expert feedback (Vuorio et al., 2022; Swamy et al., 2022b). Orthogonal offline approaches formulate imitation learning as an instrumental-variable problem to address short-range or temporally correlated confounding (Swamy et al., 2021; Zhang et al., 2020; Kumor et al., 2021; Zeng et al., 2025). As summarized in Table 1, existing causal IL methods rely on graphical adjustment, interactive expert correction, or instrumental variable, and do not account for measurement error in state observations. Our work fills this gap by leveraging the noisy measurements and deriving a estimation strategy that enable fully offline recovery of the expert policy. A more detailed discussion of related work is provided in Appendix C.

2 Model Setting and Problem Description

We study *offline* imitation learning from expert demonstrations when (i) part of the decision-relevant state is latent and affects actions with a one-step delay, and (ii) the learner only observes noisy measurements of this latent state, potentially under distribution shift between training and deployment.

We consider trajectories of length T generated by an expert interacting with an environment. At each time $t = 1, \dots, T$, the system contains:

- an observed state component $S_t \in \mathcal{S}$ (recorded in the demonstrations);
- a latent state component $U_t \in \mathcal{U}$ that is *not* recorded (and may capture unobserved physical/physiological factors, expert beliefs, internal context, etc.);
- a measurement (proxy) $W_t \in \mathcal{W}$ that is informative about U_t but may be corrupted by measurement error;
- an expert action $A_t \in \mathcal{A}$.

The learner observes demonstration data $\mathcal{D} = \{(S_{1:T}^{(i)}, W_{0:T-1}^{(i)}, A_{1:T}^{(i)})\}_{i=1}^n$, where W_{t-1} denotes the latest available proxy measurement about the *previous* latent state U_{t-1} when the decision A_t is made.¹

The expert is assumed to act (possibly approximately) to optimize an unknown objective. Concretely, there exists a reward function $r^* : \mathcal{S} \times \mathcal{A} \rightarrow \mathbb{R}$ such that the expert policy is (approximately) optimal for the induced sequential decision problem, but *neither r^* nor realized rewards are observed in the demonstrations*. This is the canonical imitation-learning regime: the learner must infer a good policy from state/measurement–action trajectories alone.

A key modeling feature is that the expert’s action at time t depends on the *current* observed state S_t and a *delayed* latent state U_{t-1} :

$$A_t \sim \pi_E(\cdot | S_t, U_{t-1}), \quad (2.1)$$

where π_E is the expert policy and U_{t-1} is unobserved to the learner. This lag captures practical situations where expert decisions depend on internal context that is formed from prior information and persists over time (see Fig. 1). Consider high-speed driving or mobile robotics on varying road surfaces. Let S_t be the current kinematic state (e.g., velocity, yaw rate, distance to obstacles) estimated from onboard sensors. Let U_t be the latent road-tire friction (or wheel–ground contact quality), which is not directly measured and changes slowly. An expert driver (or expert controller) adjusts braking/acceleration at time t using not only the current kinematics S_t but also their *current belief about friction*, which is largely inferred from the *previous* time step via wheel slip and traction signals. This yields a natural delayed dependence $U_{t-1} \rightarrow A_t$. Meanwhile, the learner only observes noisy proxies (e.g., slip ratio, traction-control activation, temperature), summarized as W_{t-1} , which can be corrupted and can vary across vehicles or weather conditions.

We model the temporal evolution through a (possibly non-linear) data-generating process in which U_t is persistent and affects future observations, and W_t is a noisy proxy of U_t . One convenient abstraction is the causal graph in Fig. 1, which implies that W_{t-1} and the recent observed history carry information about U_{t-1} , but the learner never observes U_{t-1} directly. We allow the demonstrations to be collected in one environment (training domain) and the learned policy to be deployed in another (test domain). Distribution shift may occur because the latent dynamics and/or the measurement process changes across domains (e.g., road conditions, sensor calibration, hospital protocols), even when the expert’s decision logic in (2.1) is stable. We consider settings where the variables satisfy the following conditional independences.

Assumption 2.1. *For each $t \in \{1, \dots, T\}$, let $V_{t-1} := (S_{t-1}, W_{t-1})$. The variables satisfy:*

- $S_{t-1} \perp\!\!\!\perp A_t | (S_t, U_{t-1})$ (past observed state affects A_t only through (S_t, U_{t-1})),
- $(S_{t-1}, S_t) \perp\!\!\!\perp W_{t-1} | U_{t-1}$.

2.1 Problem Description

We focus on deterministic imitation policies. For a chosen input X_t (e.g., $X_t = S_t$ or $X_t = (S_t, V_{t-1})$), a deterministic policy is a measurable map

$$\pi : \mathcal{X} \rightarrow \mathcal{A}, \quad a_t = \pi(x_t).$$

¹This indexing is appropriate in settings where proxy measurements are delayed (e.g., lab tests, batch sensor pipelines), so that W_{t-1} is available at time t while W_t becomes available only after A_t is chosen.

In this paper, we treat the expert policy $\pi_E(\cdot | S_t, U_{t-1})$ in (2.1) as an *unknown* mechanism and seek to learn a policy from demonstrations only.

A natural learner choice is to fit an observational predictor of A_t from available covariates. We consider two standard behavioral-cloning targets:

$$\begin{aligned}\pi_{\text{BC1}}(s_t) &:= \arg \max_{a \in \mathcal{A}} p(A_t = a | S_t = s_t), \\ \pi_{\text{BC2}}(s_t, v_{t-1}) &:= \arg \max_{a \in \mathcal{A}} p(A_t = a | S_t = s_t, V_{t-1} = v_{t-1}).\end{aligned}$$

Intuitively, π_{BC2} may be more predictive in-sample because V_{t-1} contains information about the delayed latent state U_{t-1} .

The following proposition formalizes the connection between deterministic BC and square-loss minimization.

Proposition 2.2 (Deterministic BC as a Bayes classifier). *Assume $\mathcal{A} = \{1, \dots, K\}$ is finite and let $e(a) \in \mathbb{R}^K$ denote the one-hot encoding of action a (i.e., $e(a)$ has a 1 in coordinate a and 0 elsewhere). Consider the one-hot squared-loss risk over deterministic policies $\pi : \mathcal{X} \rightarrow \mathcal{A}$,*

$$\mathcal{R}(\pi) := \mathbb{E}_{(X_t, A_t) \sim d_{\pi_E}} \left[\|e(A_t) - e(\pi(X_t))\|_2^2 \right].$$

Then any minimizer $\pi^ \in \arg \min_{\pi} \mathcal{R}(\pi)$ satisfies, for almost every $x \in \mathcal{X}$,*

$$\pi^*(x) \in \arg \max_{a \in \mathcal{A}} p(A_t = a | X_t = x).$$

Equivalently, $\mathcal{R}(\pi) = 2 \mathbb{E}[1 - p(A_t = \pi(X_t) | X_t)]$, so π^ maximizes the conditional success probability pointwise.*

Remark 2.3. *If one instead learns a score function $f : \mathcal{X} \rightarrow \mathbb{R}^K$ by minimizing $\mathbb{E}[\|e(A_t) - f(X_t)\|_2^2]$, the minimizer is $f^*(x) = \mathbb{E}[e(A_t) | X_t = x]$ whose coordinates equal $p(A_t = a | X_t = x)$, and the induced policy $\arg \max_a f_a^*(x)$ coincides with π^* above.*

Concerns regarding using behavioral-cloning. Despite being natural observational risk minimizers, π_{BC1} and π_{BC2} fail to directly address two questions that are central in our setting:

1. *Causal question:* how would the expert's action change if we were to intervene and set the current state to $S_t = s_t$?
2. *Deployment question:* how would the learned policy behave when deployed in an environment whose data-generating process differs from that of the training data?

The first question is not answered by observational conditionals such as $p(A_t | S_t = s_t, V_{t-1} = v_{t-1})$ because V_{t-1} may encode latent context (U_{t-1}) in a way that is correlated with S_t , producing non-causal associations. The second question becomes acute under distribution shift: even when π_{BC2} is highly predictive in the training domain, it can be brittle when the proxy channel or latent dynamics change, because it relies on observational correlations that need not be invariant.

3 A Causal Imitation Target

The concerns stated in Section 2 motivate an imitation target defined through a *counterfactual intervention*. Let $A_t^{(s)}$ denote the (potential) expert action at time t under the intervention $\text{do}(S_t = s)$, i.e., the action that would be taken if we were to set the current state to s while leaving the rest of the system to evolve naturally. For discrete actions, we define the causal-optimal imitation policy as

$$\pi_{\text{opt}}(s) := \arg \max_{a \in \mathcal{A}} p(A_t^{(s)} = a). \tag{3.1}$$

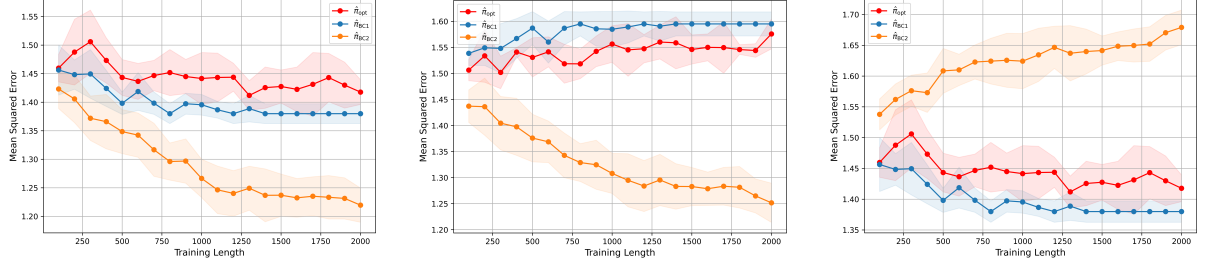


Figure 2: Mean squared error (MSE) of different policies under distributional shift with $|\mathcal{A}| = 4$. From left to right: (i) no distributional shift; (ii) shift in the proxy channel $P(U_{t-1} | S_t)$; (iii) simultaneous shifts in $P(W_{t-1} | U_{t-1})$.

(For continuous actions, one may analogously define $\pi_{\text{opt}}(s)$ as an interventional conditional mean, but we focus on the discrete form for clarity.)

We next discuss the key properties of π_{opt} , demonstrating why it is the right target for our setting.

1. Population-aggregated interpretation. The first key property is regarding the causal interpretation of π_{opt} .

Proposition 3.1. *Assume \mathcal{A} is finite and the expert follows a deterministic mechanism*

$$A_t = \pi_E(S_t, U_{t-1}).$$

Assume standard consistency for interventions and temporal ordering, so that under the intervention $\text{do}(S_t = s)$,

$$A_t^{(s)} = \pi_E(s, U_{t-1}) \quad \text{and} \quad U_{t-1}^{(s)} = U_{t-1}.$$

Then for any $s \in \mathcal{S}$ and $a \in \mathcal{A}$,

$$\begin{aligned} \mathbb{P}(A_t^{(s)} = a) &= \mathbb{P}(\pi_E(s, U_{t-1}) = a) \\ &= \mathbb{E}[\mathbb{I}\{\pi_E(s, U_{t-1}) = a\}], \end{aligned}$$

where the probability/expectation is taken over the (population) distribution of U_{t-1} . Consequently, the causal imitation target

$$\pi_{\text{opt}}(s) \in \arg \max_{a \in \mathcal{A}} \mathbb{P}(A_t^{(s)} = a)$$

admits the representation

$$\pi_{\text{opt}}(s) \in \arg \max_{a \in \mathcal{A}} \mathbb{E}[\mathbb{I}\{\pi_E(s, U_{t-1}) = a\}].$$

Corollary 3.2 (Population-aggregated interpretation). *Define the marginalized (population-aggregated) expert action distribution*

$$\pi_E(a | s) := \mathbb{P}(\pi_E(s, U_{t-1}) = a), \quad a \in \mathcal{A}.$$

Then Proposition 3.1 implies

$$\pi_{\text{opt}}(s) \in \arg \max_{a \in \mathcal{A}} \bar{\pi}_E(a | s),$$

so $\pi_{\text{opt}}(s)$ selects the action that the latent-aware expert mechanism $\pi_E(s, U_{t-1})$ chooses most frequently as U_{t-1} varies in the population. Equivalently, $\pi_{\text{opt}}(s)$ is Bayes-optimal under 0–1 loss among state-only actions:

$$\pi_{\text{opt}}(s) \in \arg \min_{a \in \mathcal{A}} \mathbb{E}[\mathbb{I}\{\pi_E(s, U_{t-1}) \neq a\}].$$

Remark 3.3. Because U_{t-1} is unobserved, a policy that conditions only on the current state s cannot, in general, reproduce the latent-aware mapping $\pi_E(s, u)$ uniformly over all latent contexts u . The representation in Proposition 3.1 shows that $\pi_{\text{opt}}(s)$ is defined by a causal quantity—the distribution of the expert’s action under the intervention $\text{do}(S_t = s)$ —rather than an observational conditional. Corollary 3.2 then provides an operational interpretation: $\pi_{\text{opt}}(s)$ is the canonical state-only summary of expert behavior, selecting the action that minimizes disagreement with $\pi_E(s, U_{t-1})$ when the latent context is drawn from its population distribution.

2. Robustness to distribution shift. The second key property is regarding robustness. Consider indexing domains by $e \in \{0, 1\}$ and write probabilities as $\mathbb{P}_e(\cdot)$. Assume the expert mechanism $\pi_E(S_t, U_{t-1})$ is invariant across domains, and assume consistency so that under $\text{do}(S_t = s)$, $A_t^{(s)} = \pi_E(s, U_{t-1})$ and $U_{t-1}^{(s)} = U_{t-1}$.

Then for any $s \in \mathcal{S}$ and $a \in \mathcal{A}$,

$$\mathbb{P}_e(A_t^{(s)} = a) = \sum_{u \in \mathcal{U}} \mathbb{I}\{\pi_E(s, u) = a\} \mathbb{P}_e(U_{t-1} = u), \quad (3.2)$$

so the target $\pi_{\text{opt}}^{(e)}(s) \in \arg \max_{a \in \mathcal{A}} \mathbb{P}_e(A_t^{(s)} = a)$ depends on the domain only through the *marginal* distribution $\mathbb{P}_e(U_{t-1})$ (and the invariant mechanism π_E).

Robustness relative to π_{BC2} . The BC2 target is $\pi_{\text{BC2}}^{(e)}(s, v) \in \arg \max_{a \in \mathcal{A}} \mathbb{P}_e(A_t = a \mid S_t = s, V_{t-1} = v)$, with $V_{t-1} = (S_{t-1}, W_{t-1})$. Because W_{t-1} is generated through the measurement channel $\mathbb{P}_e(W_{t-1} \mid U_{t-1})$, the posterior $\mathbb{P}_e(U_{t-1} \mid S_t = s, V_{t-1} = v)$ and hence $\mathbb{P}_e(A_t \mid S_t, V_{t-1})$ are direct functionals of $\mathbb{P}_e(W_{t-1} \mid U_{t-1})$. Therefore, a change in the measurement mechanism across domains can change $\pi_{\text{BC2}}^{(e)}$ even when π_E is invariant. In contrast, (3.2) shows that $\pi_{\text{opt}}^{(e)}$ does *not* involve $\mathbb{P}_e(W_{t-1} \mid U_{t-1})$ at all; in particular, if $\mathbb{P}_0(U_{t-1}) = \mathbb{P}_1(U_{t-1})$ and only $\mathbb{P}_e(W_{t-1} \mid U_{t-1})$ changes, then $\mathbb{P}_0(A_t^{(s)}) = \mathbb{P}_1(A_t^{(s)})$ for all s and hence $\pi_{\text{opt}}^{(0)} = \pi_{\text{opt}}^{(1)}$.

Robustness relative to π_{BC1} . The BC1 target is $\pi_{\text{BC1}}^{(e)}(s) \in \arg \max_{a \in \mathcal{A}} \mathbb{P}_e(A_t = a \mid S_t = s)$, and under $A_t = \pi_E(S_t, U_{t-1})$ we can write $\mathbb{P}_e(A_t = a \mid S_t = s) = \sum_{u \in \mathcal{U}} \mathbb{I}\{\pi_E(s, u) = a\} \mathbb{P}_e(U_{t-1} = u \mid S_t = s)$. Thus $\pi_{\text{BC1}}^{(e)}$ depends on $\mathbb{P}_e(U_{t-1} \mid S_t = s)$, which is sensitive to the environment dynamics. In particular, by Bayes’ rule, $\mathbb{P}_e(U_{t-1} = u \mid S_t = s) \propto \mathbb{P}_e(S_t = s \mid U_{t-1} = u) \mathbb{P}_e(U_{t-1} = u)$, and the conditional likelihood $\mathbb{P}_e(S_t \mid U_{t-1})$ is a functional of the state and latent transition kernels, e.g. $\mathbb{P}_e(S_t \mid U_t, U_{t-1}, S_{t-1}, A_{t-1})$ and $\mathbb{P}_e(U_t \mid U_{t-1}, S_{t-1}, A_{t-1})$, together with the induced distribution of (S_{t-1}, A_{t-1}) under the data-generating process. Therefore, changes in these kernels can alter $\mathbb{P}_e(U_{t-1} \mid S_t = s)$ and hence the BC targets, even if the marginal $\mathbb{P}_e(U_{t-1})$ remains (approximately) the same.

By contrast, (3.2) shows that $\pi_{\text{opt}}^{(e)}$ depends on the same dynamics only through the marginal $\mathbb{P}_e(U_{t-1})$. In particular, if a shift changes the kernels $\mathbb{P}_e(S_t \mid U_t, U_{t-1}, S_{t-1}, A_{t-1})$ and/or $\mathbb{P}_e(U_t \mid U_{t-1}, S_{t-1}, A_{t-1})$ but preserves the marginal of the delayed latent context, $\mathbb{P}_0(U_{t-1}) \approx \mathbb{P}_1(U_{t-1})$, then π_{opt} is approximately invariant. Formally, for any s and a ,

$$\left| \mathbb{P}_0(A_t^{(s)} = a) - \mathbb{P}_1(A_t^{(s)} = a) \right| \leq \|\mathbb{P}_0(U_{t-1}) - \mathbb{P}_1(U_{t-1})\|_1.$$

Consequently, whenever the action-probability gap in $\mathbb{P}_e(A_t^{(s)} = \cdot)$ is larger than the induced perturbation above, the $\arg \max$ defining $\pi_{\text{opt}}^{(e)}(s)$ is unchanged across domains. Finally, it is entirely possible for the transition kernels to change while keeping $\mathbb{P}(U_{t-1})$ approximately fixed; for example, distinct Markov transition kernels can share (exactly or approximately) the same stationary distribution, so changes in dynamics need not imply large changes in the marginal prevalence of U .

Figure 2 provides empirical support for the robustness analysis above in terms of mean squared error (MSE) (i.e., compares the actions selected by the learned policy to those of the expert) as defined in Section 6. When the channel $\mathbb{P}_e(U_{t-1} \mid S_t)$ is perturbed (through a shift changes the kernels $\mathbb{P}_e(S_t \mid U_t, U_{t-1}, S_{t-1}, A_{t-1})$), the performance of π_{BC1} degrades noticeably relative to the no-shift case, reflecting its explicit dependence on $\mathbb{P}_e(U_{t-1} \mid S_t = s)$, while π_{opt} remains essentially invariant. In contrast, when the measurement mechanism

$\mathbb{P}_e(W_{t-1} | U_{t-1})$ is altered, π_{BC2} exhibits a clear performance drop, consistent with the fact that its target depends on the posterior $\mathbb{P}_e(U_{t-1} | S_t, V_{t-1})$, which is a direct functional of $\mathbb{P}_e(W_{t-1} | U_{t-1})$. The details of the data-generating process is provided in Appendix D. Overall, the results confirm that π_{BC1} is more sensitive to shifts in $\mathbb{P}_e(U_{t-1} | S_t)$, whereas π_{BC2} is vulnerable to changes in the measurement channel, while π_{opt} remains robust across all considered shifts.

3.1 Comparison Between π_{opt} and BC

Under our model, the expert follows a latent-aware mechanism $A_t = \pi_E(S_t, U_{t-1})$, while the learner only observes (S_t, V_{t-1}) with $V_{t-1} = (S_{t-1}, W_{t-1})$. Behavioral cloning targets are *observational*: $\pi_{BC1}(s)$ and $\pi_{BC2}(s, v)$ maximize conditional action probabilities under the training distribution, which (under determinism) can be written as conditional averages of the latent-aware expert rule with respect to the distribution of the latent context given observed covariates (e.g., $\mathcal{L}(U_{t-1} | S_t = s)$ or $\mathcal{L}(U_{t-1} | S_t = s, V_{t-1} = v)$). In contrast, $\pi_{opt}(s)$ is defined via the interventional response $\mathbb{P}(A_t^{(s)} = \cdot)$ and averages $\pi_E(s, U_{t-1})$ with respect to the *marginal* distribution of U_{t-1} . Since conditioning on S_t or (S_t, V_{t-1}) typically changes the latent distribution whenever U_{t-1} is statistically associated with these covariates, the resulting observational and interventional targets generally disagree; moreover, $\pi_{BC2}(s, v)$ can vary with v and therefore need not coincide with a state-only target. In the Appendix, we give a simple data-generating process in which π_{BC1} , π_{BC2} , and π_{opt} yield different decision boundaries even in the population. They coincide only under strong (and typically unrealistic) conditions, summarized in Proposition 3.4.

Proposition 3.4 (Rare coincidence of BC targets and π_{opt}). *Assume a finite action space \mathcal{A} and a deterministic expert mechanism $A_t = \pi_E(S_t, U_{t-1})$. For each $s \in \mathcal{S}$ and $a \in \mathcal{A}$, define the action-induced latent sets*

$$B_a(s) := \{u \in \mathcal{U} : \pi_E(s, u) = a\}.$$

Then, up to arbitrary tie-breaking,

$$\begin{aligned} \pi_{opt}(s) &\in \arg \max_{a \in \mathcal{A}} \mathbb{P}(U_{t-1} \in B_a(s)), \\ \pi_{BC1}(s) &\in \arg \max_{a \in \mathcal{A}} \mathbb{P}(U_{t-1} \in B_a(s) | S_t = s), \\ \pi_{BC2}(s, v) &\in \arg \max_{a \in \mathcal{A}} \mathbb{P}(U_{t-1} \in B_a(s) | S_t = s, V_{t-1} = v). \end{aligned}$$

Moreover, the following sufficient conditions guarantee coincidence:

1. *If $U_{t-1} \perp\!\!\!\perp S_t$, then $\pi_{BC1}(s) = \pi_{opt}(s)$ for all s (up to ties).*
2. *If $U_{t-1} \perp\!\!\!\perp (S_t, V_{t-1})$, then $\pi_{BC2}(s, v) = \pi_{opt}(s)$ for all (s, v) (up to ties).*

In particular, unless conditioning on S_t (or (S_t, V_{t-1})) leaves the induced action probabilities $\mathbb{P}(U_{t-1} \in B_a(s))$ unchanged—as in the independence cases above, or in degenerate cases where $\pi_E(s, u)$ is (essentially) constant in u —the BC targets and π_{opt} are generally different.

4 Identification of the Optimal Policy

So far, we observed that in IL with measurement error and distribution shift, π_{opt} is a desirable target. We now ask when this policy is identifiable from purely observational expert demonstrations. Our identification strategy is inspired by the proximal causal inference (PCI) framework (Miao et al., 2018; Tchetgen Tchetgen et al., 2020) and, in particular, its longitudinal extension for complex longitudinal studies (Ying et al., 2023). While PCI is often presented for identifying causal effects on outcome means, our goal is to identify the *full interventional distribution* of the expert’s action. The key to proximal identification is access to two proxy variables for U_{t-1} . (Ying et al., 2023) consider a setting with a single “end of the study” outcome variable, which is affected by latent confounders at previous time points, and assume each latent confounder has two

distinct proxy variables. On the other hand, we have one action variable (which is the variable that we are interested in its potential outcomes) at every time point. We set the lagged state $Z_t := S_{t-1}$ to play the role of a *treatment-inducing proxy*, and the noisy measurement W_{t-1} to play the role of an *outcome-inducing proxy*. Notably, the *same* state process appears at two time indices: S_{t-1} is used as a proxy for the delayed confounder U_{t-1} , while S_t is the variable we conceptually intervene on. This time-indexed “reuse” is what makes it possible to identify $p(A_t^{(s)})$ despite unobserved confounding. We require the following core assumptions:

Assumption 4.1 (Consistency). *For all t and all s in the support of S_t , we have $S_t = s \implies A_t = A_t^{(s)}$ a.s.*

Assumption 4.2 (Positivity). *For all t , all u in the support of U_{t-1} , and all s in the support of S_t , we have $p(S_t = s \mid U_{t-1} = u) > 0$.*

Assumption 4.3 (Latent exchangeability). *For all t and all s , we have $A_t^{(s)} \perp\!\!\!\perp S_t \mid U_{t-1}$.*

Assumptions 4.1 and 4.2 are standard. Assumption 4.3 is a significantly weaker version of the standard conditional exchangeability: it posits that, once one conditions on the *unobserved* confounder U_{t-1} , the counterfactual action under $\text{do}(S_t = s)$ is independent of the realized state S_t .

4.1 Discrete Case: Identification via Matrix Inversion

Assume $Z_t := S_{t-1}$, W_{t-1} , U_{t-1} and A_t are categorical. For a fixed observed state s , define the matrices $P_{A|Z,s} \in \mathbb{R}^{|\mathcal{A}| \times |\mathcal{Z}|}$, $P_{W|Z,s} \in \mathbb{R}^{|\mathcal{W}| \times |\mathcal{Z}|}$, and $P_W \in \mathbb{R}^{|\mathcal{W}|}$, with entries

$$\begin{aligned} [P_{A|Z,s}]_{a,z} &:= p(A_t = a \mid S_{t-1} = z, S_t = s), \\ [P_{W|Z,s}]_{w,z} &:= p(W_{t-1} = w \mid S_{t-1} = z, S_t = s), \\ [P_W]_w &:= p(W_{t-1} = w). \end{aligned}$$

Assumption 4.4. *Let $k := |U_{t-1}|$. Assume $|\mathcal{Z}| \geq k$ and $|\mathcal{W}| \geq k$, and for every s in the support of S_t , the matrix $P_{W|Z,s}$ has rank k . Equivalently, for each such s there exist coarsenings Z'_t of S_{t-1} and W'_{t-1} of W_{t-1} taking values in $\{1, \dots, k\}$ such that $P_{W'|Z',s}$ is square and invertible.*

Roughly speaking, Assumption 4.4 requires S_{t-1} and W_{t-1} to be sufficiently informative about U_{t-1} .

Theorem 4.5. *Under Assumptions 2.1, 4.1 - 4.4, the interventional action distribution is identified. In particular, for any s and any coarsenings (Z'_t, W'_{t-1}) that make $P_{W'|Z',s}$ invertible,*

$$P(A_t^{(s)}) = P_{A|Z',s} \left(P_{W'|Z',s} \right)^{-1} P_W,$$

where $P(A_t^{(s)}) \in \mathbb{R}^{|\mathcal{A}|}$ denotes the vector with entries $p(A_t^{(s)} = a)$. Consequently, $\pi_{\text{opt}}(s) \in \arg \max_{a \in \mathcal{A}} p(A_t^{(s)} = a)$ is identified for all s (up to ties).

4.2 Continuous Case: Identification via a Confounding Bridge

We now present the identification result for the continuous case by assuming the following completeness and confounding bridge assumptions which ensures that S and W contain sufficient variation to recover functions of the latent state.

Assumption 4.6 (Completeness). *For each s in the support of S_t , for any square-integrable function ν , if $\mathbb{E}[\nu(U_{t-1}) \mid S_{t-1}, S_t = s] = 0$ a.s., then $\nu(U_{t-1}) = 0$ a.s.*

Assumption 4.7 (Confounding bridge). *For each action $a \in \mathcal{A}$, there exists a function $h_a : \mathcal{W} \times \mathcal{S} \rightarrow \mathbb{R}$ such that for all s in the support of S_t and all z in the support of S_{t-1} ,*

$$\begin{aligned} p(A_t = a \mid S_{t-1} = z, S_t = s) \\ = \int h_a(w, s) p(w \mid S_{t-1} = z, S_t = s) dw. \end{aligned} \quad (4.1)$$

Equation (4.1) is a Fredholm integral equation of the first kind. The solution links observed and counterfactual distribution. and solutions need not be unique in general.

Theorem 4.8. *Under Assumptions 2.1, 4.1, 4.2, 4.3, 4.6, and 4.7, the interventional action probabilities are identified by*

$$p\left(A_t^{(s)} = a\right) = \int h_a(w, s) p(w) dw, \quad a \in \mathcal{A}. \quad (4.2)$$

Consequently, $\pi_{\text{opt}}(s) \in \arg \max_{a \in \mathcal{A}} p(A_t^{(s)} = a)$ is identified for all s (up to ties).

Equipped with the identification results in Theorems 4.5 and 4.8, the next section develops estimation procedures for π_{opt} in both continuous and discrete regimes.

5 Estimation of the Optimal Policy

This section describes how to estimate the causal-optimal imitation policy $\pi_{\text{opt}}(s)$ from offline expert demonstrations. We assume we observe n expert trajectories of length T , $\mathcal{D}_E = \{(S_{1:T}^{(i)}, W_{0:T-1}^{(i)}, A_{1:T}^{(i)})\}_{i=1}^n$, and we form the pooled sample of tuples $\mathcal{I} := \{(Z_t^{(i)}, S_t^{(i)}, W_{t-1}^{(i)}, A_t^{(i)}) : i = 1, \dots, n, t = 1, \dots, T\}$, where $Z_t = S_{t-1}$.

5.1 Discrete Case: Plug-in Estimator with Coarsenings

Assume $\mathcal{S}, \mathcal{W}, \mathcal{A}$ are finite. As discussed in Section 4, identification only requires *some* pair of coarsenings $Z'_t = \phi_Z(Z_t) \in \{1, \dots, m\}$, $W'_{t-1} = \phi_W(W_{t-1}) \in \{1, \dots, m\}$, such that, for each $s \in \mathcal{S}$, the matrix $P_{W'|Z',s} \in \mathbb{R}^{m \times m}$ is invertible. Equivalently, we require $|\mathcal{Z}'| = |\mathcal{W}'| = m$ and $\det(P_{W'|Z',s}) \neq 0$. For each $s \in \mathcal{S}$, estimate by empirical frequencies $\widehat{P}_{A|Z',s} \in \mathbb{R}^{|\mathcal{A}| \times m}$, $\widehat{P}_{W'|Z',s} \in \mathbb{R}^{m \times m}$, $\widehat{p}_{W'} \in \mathbb{R}^m$. The discrete identification formula yields the natural plug-in estimator

$$\widehat{p}(A_t^{(s)}) = \widehat{P}_{A|Z',s} \widehat{P}_{W'|Z',s}^{-1} \widehat{p}_{W'} \in \mathbb{R}^{|\mathcal{A}|}. \quad (5.1)$$

Finally, define $\widehat{\pi}_{\text{opt}}(s) := \arg \max_{a \in \mathcal{A}} \widehat{p}(A_t^{(s)} = a)$, where $\widehat{p}(A_t^{(s)} = a)$ is the a -th coordinate of $\widehat{p}(A_t^{(s)})$.

5.2 Continuous Case: RKHS-Adversarial Estimation

Now assume states take values in continuous spaces. For simplicity, suppose $\mathcal{A} = \{1, \dots, K\}$ is finite and define the one-vs-all labels $Y_t^{(a)} := \mathbb{I}\{A_t = a\}$ for each $a \in \mathcal{A}$. The continuous identification result in Section 4 implies that it suffices to estimate, for each a , a bridge function $h_a : \mathcal{W} \times \mathcal{S} \rightarrow \mathbb{R}$ satisfying the conditional moment restriction $\mathbb{E}[Y_t^{(a)} - h_a(W_{t-1}, S_t) \mid Z_t, S_t] = 0$, a.s. Given such h_a , the causal action probability is

$$p(A_t^{(s)} = a) = \int h_a(w, s) p(w) dw = \mathbb{E}[h_a(W_{t-1}, s)], \quad (5.2)$$

and therefore $\pi_{\text{opt}}(s) = \arg \max_{a \in \mathcal{A}} \mathbb{E}[h_a(W_{t-1}, s)]$.

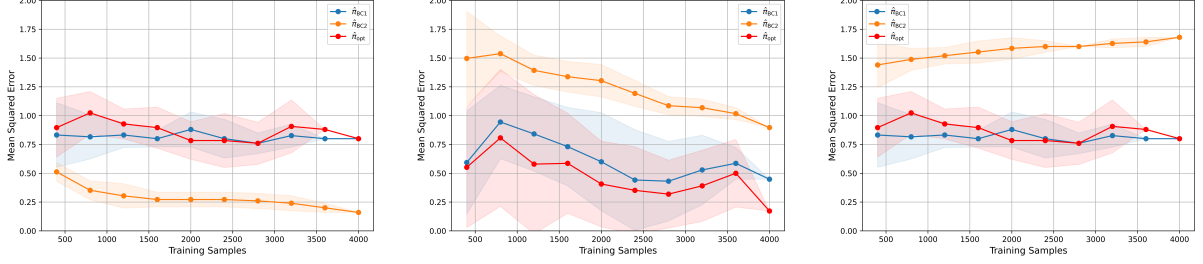


Figure 3: Mean squared error (MSE) of different policies under distributional shift. From left to right: (i) no distributional shift; (ii) shift in ICU time and lactate level; (iii) simultaneous shifts in $P(W_{t-1} | U_{t-1})$. Red corresponds to $\hat{\pi}_{\text{opt}}$, orange to $\hat{\pi}_{\text{BC1}}$, and green to $\hat{\pi}_{\text{BC2}}$.

Regularized minimax estimator. Following minimax/RKHS approach (Ghassami et al., 2022; Dikkala et al., 2020) for solving integral equations in proximal causal inference, we estimate h_a by the regularized saddle-point problem

$$\begin{aligned} \hat{h}_a \in \arg \min_{h \in \mathcal{H}} \sup_{q \in \mathcal{Q}} & \left\{ \widehat{\mathbb{E}} \left[(Y^{(a)} - h(W, S)) q(Z, S) \right. \right. \\ & \left. \left. - q(Z, S)^2 \right] - \lambda_Q \|q\|_{\mathcal{Q}}^2 + \lambda_H \|h\|_{\mathcal{H}}^2 \right\}, \end{aligned} \quad (5.3)$$

where $\widehat{\mathbb{E}}$ denotes the empirical average over the pooled tuples in \mathcal{I} , \mathcal{H} is an RKHS over $\mathcal{W} \times \mathcal{S}$ (for h), \mathcal{Q} is an RKHS over $\mathcal{Z} \times \mathcal{S}$ (for q), and $\lambda_Q, \lambda_H > 0$ are regularization parameters. The regularization parameters control the smoothness of the estimators that can be tuned via cross validation on projected error (see (Ghassami et al., 2022; Dikkala et al., 2020)).

Let $N := |\mathcal{I}| = nT$ be the number of pooled tuples and index them by $j = 1, \dots, N$, writing (Z_j, S_j, W_j, A_j) and $Y_j^{(a)} = \mathbb{I}\{A_j = a\}$. Let $K_H \in \mathbb{R}^{N \times N}$ and $K_Q \in \mathbb{R}^{N \times N}$ be the empirical kernel matrices $(K_H)_{ij} = K_{\mathcal{H}}((W_i, S_i), (W_j, S_j))$, $(K_Q)_{ij} = K_{\mathcal{Q}}((Z_i, S_i), (Z_j, S_j))$, and define $\Gamma := \frac{1}{4} K_Q \left(\frac{1}{N} K_Q + \lambda_Q I_N \right)^{-1}$.

Proposition 5.1 (Closed-form solution). *Assume \mathcal{H} and \mathcal{Q} are RKHSs and consider (5.3). Then \hat{h}_a admits a representer*

$$\hat{h}_a(w, s) = \sum_{j=1}^N \alpha_{a,j} K_{\mathcal{H}}((W_j, S_j), (w, s))$$

for coefficient vector $\alpha_a \in \mathbb{R}^N$ defined as

$$\alpha_a = (K_H \Gamma K_H + N^2 \lambda_H K_H)^{\dagger} K_H \Gamma y_a, \quad (5.4)$$

where $y_a := (Y_1^{(a)}, \dots, Y_N^{(a)})^{\top}$ and $(\cdot)^{\dagger}$ denotes the Moore–Penrose pseudoinverse.

Given \hat{h}_a , we estimate (5.2) by the empirical plug-in $\hat{p}(A_t^{(s)} = a) := \frac{1}{N} \sum_{j=1}^N \hat{h}_a(W_j, s)$, $a \in \mathcal{A}$, and return $\hat{\pi}_{\text{opt}}(s) := \arg \max_{a \in \mathcal{A}} \hat{p}(A_t^{(s)} = a)$.

A pseudocode covering both the discrete and continuous estimators is presented in Algorithm 1.

6 Experiments

6.1 Simulation study

We generate n expert trajectories of length T from the model in Section 2. In simulation, the full data include latent variables, $\{(S_{1:T}^{(i)}, W_{0:T-1}^{(i)}, U_{0:T-1}^{(i)}, A_{1:T}^{(i)})\}_{i=1}^n$, but the learner observes only (S_t, W_{t-1}, A_t) . We

Algorithm 1 **CausIL**: Estimating π_{opt} (discrete or continuous)

Require: Expert trajectories $\mathcal{D}_E = \{(S_{1:T}^{(i)}, W_{0:T-1}^{(i)}, A_{1:T}^{(i)})\}_{i=1}^n$; mode $\in \{\text{DISCRETE}, \text{CONTINUOUS}\}$.
Ensure: Estimated policy $\widehat{\pi}_{\text{opt}}(\cdot)$.

- 1: Form pooled tuples $\mathcal{I} = \{(Z_t^{(i)}, S_t^{(i)}, W_{t-1}^{(i)}, A_t^{(i)})\}$ with $Z_t := S_{t-1}$; let $N := |\mathcal{I}|$.
- 2: **if** mode = DISCRETE **then**
- 3: Choose coarsenings $Z'_t = \phi_Z(Z_t)$ and $W'_{t-1} = \phi_W(W_{t-1})$ such that $\widehat{P}_{W'|Z',s}$ is invertible for each $s \in \mathcal{S}$.
- 4: **for** each $s \in \mathcal{S}$ **do**
- 5: Estimate $\widehat{P}_{A|Z',s}$, $\widehat{P}_{W'|Z',s}$, and $\widehat{p}_{W'}$ by empirical frequencies over \mathcal{I} .
- 6: Compute $\widehat{p}(A^{(s)}) \leftarrow \widehat{P}_{A|Z',s} \widehat{P}_{W'|Z',s}^{-1} \widehat{P}_{W'}$. (Eq. (5.1))
- 7: Set $\widehat{\pi}_{\text{opt}}(s) \leftarrow \arg \max_{a \in \mathcal{A}} \widehat{p}(A^{(s)} = a)$.
- 8: **end for**
- 9: **else**
- 10: Fix RKHSs \mathcal{H} on $\mathcal{W} \times \mathcal{S}$ and \mathcal{Q} on $\mathcal{Z} \times \mathcal{S}$, with kernels $K_{\mathcal{H}}, K_{\mathcal{Q}}$ and regularization $\lambda_H, \lambda_Q > 0$.
- 11: Build kernel matrices $K_H, K_Q \in \mathbb{R}^{N \times N}$ over \mathcal{I} and compute $\Gamma \leftarrow \frac{1}{4} K_Q \left(\frac{1}{N} K_Q + \lambda_Q I_N \right)^{-1}$.
- 12: **for** each action $a \in \mathcal{A}$ **do**
- 13: Set $y_a[j] \leftarrow \mathbb{I}\{A_j = a\}$ for pooled index $j = 1, \dots, N$.
- 14: Compute $\alpha_a \leftarrow (K_H \Gamma K_H + N^2 \lambda_H K_H)^\dagger K_H \Gamma y_a$. (Eq. (5.4))
- 15: Define $\widehat{h}_a(w, s) \leftarrow \sum_{j=1}^N \alpha_{a,j} K_{\mathcal{H}}((W_j, S_j), (w, s))$. (Proposition 5.1)
- 16: **end for**
- 17: For a query s , compute $\widehat{p}(A^{(s)} = a) \leftarrow \frac{1}{N} \sum_{j=1}^N \widehat{h}_a(W_j, s)$ for all $a \in \mathcal{A}$.
- 18: Set $\widehat{\pi}_{\text{opt}}(s) \leftarrow \arg \max_{a \in \mathcal{A}} \widehat{p}(A^{(s)} = a)$.
- 19: **end if**

pool decision-time tuples $\mathcal{I} := \{(Z_t^{(i)}, S_t^{(i)}, W_{t-1}^{(i)}, A_t^{(i)}) : i = 1, \dots, n, t = 1, \dots, T\}$, with $Z_t := S_{t-1}$, and all variables are categorical (with possibly different cardinalities). Briefly, W_{t-1} is generated from U_{t-1} , the latent state evolves as a function of $(U_{t-1}, S_{t-1}, A_{t-1})$, the observed state depends on $(U_t, U_{t-1}, S_{t-1}, A_{t-1})$, and the expert acts according to $A_t = \pi_E(S_t, U_{t-1})$. Exact functional forms and parameters are reported in the appendix.

We vary the training size from $N = 100$ to $N = 1000$ and evaluate on a fixed test set of $N_{\text{test}} = 1000$. As mentioned in Section 2, we consider two types of test-time shift: (i) *measurement shift* in the proxy channel $p(W_{t-1} | U_{t-1})$, and (ii) *dynamics shift* in the state/latent transition mechanisms. Performance is measured by the mean squared one-hot imitation loss

$$\text{MSE}(\widehat{\pi}) = \frac{1}{N_{\text{test}}} \sum_{j=1}^{N_{\text{test}}} \|e(A_j) - e(\widehat{\pi}(X_j))\|_2^2,$$

where (X_j, A_j) are test tuples (with $X_j = S_t$ for BC1/**CausIL** and $X_j = (S_t, V_{t-1})$ for BC2), and $e(\cdot)$ is the one-hot encoding. Fig. 2 summarizes results: **CausIL** is robust to measurement shift and, under dynamics shifts that preserve the marginal prevalence of the delayed latent context, is empirically more stable than BC baselines.

6.2 Real-Data Experiment

We evaluate on the PhysioNet/Computing in Cardiology Challenge 2019 cohort (Reyna et al., 2020), which provides hourly ICU time series of vital signs and laboratory measurements from multiple hospitals. Because the released data do not include explicit clinician intervention actions (e.g., fluids or vasopressors), we construct a *semi-simulated* imitation task using real covariate trajectories and simulated expert actions.

We define the observed state using a set of routinely monitored vitals, $S_t = (\text{HR}_t, \text{MAP}_t, \text{O2Sat}_t, \text{Resp}_t, \text{Temp}_t)$, and treat lactate as a delayed latent context $U_t := \text{Lactate}_t$ that reflects underlying perfusion/severity but is typically incorporated with delay (e.g., due to lab turnaround and charting). We simulate a three-level ‘‘hemodynamic support intensity’’ action $A_t \in \{0, 1, 2\}$ (no escalation / moderate escalation / aggressive escalation) via an expert rule $A_t = \pi_E(S_t, U_{t-1})$, and provide the learner a noisy proxy W_{t-1} of U_{t-1} . To study robustness, we induce (i) *population shift* by constructing a test cohort with systematically different trajectory composition (e.g., longer stays and higher lactate prevalence), and (ii) *measurement shift* by changing the noise/bias in the measurement mechanism $p(W_{t-1} | U_{t-1})$ between train and test. Full preprocessing and simulation details are in Appendix E.

Fig. 3 reports imitation error under both shift types. BC baselines exhibit increased error and variability under population shift, and BC2 degrades sharply under measurement shift due to reliance on the measurement mechanism. In contrast, **CausIL** attains lower error and remains stable across training sizes.

7 Conclusion

We studied offline imitation learning under state measurement error and distribution shift, and showed that BC can converge to systematically biased policies because it relies on non-invariant observational state–action correlations. To address this, we proposed a causal imitation framework establishing identification conditions for a causal-optimal target policy and developing estimators for both discrete and continuous settings. Across simulation studies and a semi-simulated ICU decision-making task built from the PhysioNet/Computing in Cardiology Challenge 2019 cohort, **CausIL** consistently achieved lower imitation error and exhibited markedly improved stability under measurement-mechanism and population shifts relative to BC baselines. These results highlight the importance of targeting interventional quantities when learning policies from purely observational demonstrations in realistic, shifting environments.

References

Dean A. Pomerleau. ALVINN: An autonomous land vehicle in a neural network. In *Advances in Neural Information Processing Systems 1*, 1989.

Andrew Y. Ng and Stuart J. Russell. Algorithms for inverse reinforcement learning. In *Proceedings of the Seventeenth International Conference on Machine Learning (ICML)*, pages 663–670, 2000.

Jonathan Ho and Stefano Ermon. Generative adversarial imitation learning. In *Advances in Neural Information Processing Systems 29 (NeurIPS 2016)*, pages 4565–4573, 2016a.

Pim de Haan, Dinesh Jayaraman, and Sergey Levine. Causal confusion in imitation learning. In *Advances in Neural Information Processing Systems 32 (NeurIPS 2019)*, pages 11693–11704, 2019.

Junzhe Zhang, Daniel Kumor, and Elias Bareinboim. Causal imitation learning with unobserved confounders. In *Advances in Neural Information Processing Systems 33 (NeurIPS 2020)*, 2020.

Daniel Kumor, Junzhe Zhang, and Elias Bareinboim. Sequential causal imitation learning with unobserved confounders. In *Advances in Neural Information Processing Systems 34 (NeurIPS 2021)*, pages 14669–14680, 2021.

Gokul Swamy, Sanjiban Choudhury, Drew Bagnell, and Steven Wu. Causal imitation learning under temporally correlated noise. In *International Conference on Machine Learning*, pages 20877–20890. PMLR, 2022a.

Gokul Swamy, Sanjiban Choudhury, J Bagnell, and Steven Z Wu. Sequence model imitation learning with unobserved contexts. *Advances in Neural Information Processing Systems*, 35:17665–17676, 2022b.

Yan Zeng, Shenglan Nie, Feng Xie, Libo Huang, Peng Wu, and Zhi Geng. Confounded causal imitation learning with instrumental variables. *arXiv preprint arXiv:2507.17309*, 2025.

Daqian Shao, Thomas Kleine Buening, and Marta Kwiatkowska. A unifying framework for causal imitation learning with hidden confounders. *arXiv preprint arXiv:2502.07656*, 2025.

Wang Miao, Zhi Geng, and Eric J Tchetgen Tchetgen. Identifying causal effects with proxy variables of an unmeasured confounder. *Biometrika*, 105(4):987–993, 2018.

Eric J Tchetgen Tchetgen, Andrew Ying, Yifan Cui, Xu Shi, and Wang Miao. An introduction to proximal causal learning. *arXiv preprint arXiv:2009.10982*, 2020.

Stéphane Ross, Geoffrey J. Gordon, and J. Andrew Bagnell. A reduction of imitation learning and structured prediction to no-regret online learning. In *Proceedings of the Fourteenth International Conference on Artificial Intelligence and Statistics (AISTATS)*, volume 15 of *Proceedings of Machine Learning Research*, pages 627–635. PMLR, 2011.

Guy Tennenholtz, Uri Shalit, and Shie Mannor. Off-policy evaluation in partially observable environments. In *Proceedings of the AAAI Conference on Artificial Intelligence*, volume 34, pages 10276–10283, 2020.

Chengchun Shi, Masatoshi Uehara, Jiawei Huang, and Nan Jiang. A minimax learning approach to off-policy evaluation in confounded partially observable markov decision processes. In *Proceedings of the 39th International Conference on Machine Learning (ICML)*, volume 162 of *Proceedings of Machine Learning Research*, pages 20057–20094. PMLR, 2022.

Rui Miao, Zhengling Qi, and Xiaoke Zhang. Off-policy evaluation for episodic partially observable markov decision processes under non-parametric models. *Advances in Neural Information Processing Systems*, 35: 593–606, 2022.

Chengchun Shi, Jin Zhu, Ye Shen, Shikai Luo, Hongtu Zhu, and Rui Song. Off-policy confidence interval estimation with confounded markov decision process. *Journal of the American Statistical Association*, 119(545):273–284, 2024.

Mao Hong, Zhengling Qi, and Yanxun Xu. Model-based reinforcement learning for confounded pomdps. In *Forty-first International Conference on Machine Learning*, 2024.

Andrew Bennett and Nathan Kallus. Proximal reinforcement learning: Efficient off-policy evaluation in partially observed markov decision processes. *Operations Research*, 72(3):1071–1086, 2024a. doi: 10.1287/opre.2021.0781.

Pim De Haan, Dinesh Jayaraman, and Sergey Levine. Causal confusion in imitation learning. *Advances in neural information processing systems*, 32, 2019.

Pedro A. Ortega, Markus Kunesch, Grégoire Delétang, Tim Genewein, Jordi Grau-Moya, Joel Veness, Jonas Buchli, Jonas Degrave, Bilal Piot, Julien Perolat, Tom Everitt, Corentin Tallec, Emilio Parisotto, Tom Erez, Yutian Chen, Scott Reed, Marcus Hutter, Nando de Freitas, and Shane Legg. Shaking the foundations: delusions in sequence models for interaction and control, 2021.

Risto Vuorio, Pim De Haan, Johann Brehmer, Hanno Ackermann, Daniel Dijkman, and Taco Cohen. Deconfounded imitation learning. In *Deep Reinforcement Learning Workshop NeurIPS 2022*, 2022.

Gokul Swamy, Sanjiban Choudhury, J Andrew Bagnell, and Steven Wu. Of moments and matching: A game-theoretic framework for closing the imitation gap. In *International Conference on Machine Learning*, pages 10022–10032. PMLR, 2021.

Andrew Ying, Wang Miao, Xu Shi, and Eric J Tchetgen Tchetgen. Proximal causal inference for complex longitudinal studies. *Journal of the Royal Statistical Society Series B: Statistical Methodology*, 85(3):684–704, 2023.

AmirEmad Ghassami, Andrew Ying, Ilya Shpitser, and Eric Tchetgen Tchetgen. Minimax kernel machine learning for a class of doubly robust functionals with application to proximal causal inference. In *International conference on artificial intelligence and statistics*, pages 7210–7239. PMLR, 2022.

Nishanth Dikkala, Greg Lewis, Lester Mackey, and Vasilis Syrgkanis. Minimax estimation of conditional moment models. *Advances in Neural Information Processing Systems*, 33:12248–12262, 2020.

Matthew A Reyna, Christopher S Josef, Russell Jeter, Supreeth P Shashikumar, M Brandon Westover, Shamim Nemati, Gari D Clifford, and Ashish Sharma. Early prediction of sepsis from clinical data: the physionet/computing in cardiology challenge 2019. *Critical care medicine*, 48(2):210–217, 2020.

Dean A Pomerleau. Alvinn: An autonomous land vehicle in a neural network. *Advances in neural information processing systems*, 1, 1988.

Yann LeCun, Sumit Chopra, Raia Hadsell, M Ranzato, Fujie Huang, et al. A tutorial on energy-based learning. *Predicting structured data*, 1(0), 2006.

Stuart Russell. Learning agents for uncertain environments. In *Proceedings of the eleventh annual conference on Computational learning theory*, pages 101–103, 1998.

Jonathan Ho and Stefano Ermon. Generative adversarial imitation learning. *Advances in neural information processing systems*, 29, 2016b.

Stephane Ross and J Andrew Bagnell. Reinforcement and imitation learning via interactive no-regret learning. *arXiv preprint arXiv:1406.5979*, 2014.

Andrew Bennett and Nathan Kallus. Proximal reinforcement learning: Efficient off-policy evaluation in partially observed markov decision processes. *Operations Research*, 72(3):1071–1086, 2024b.

Samuel Pfrommer, Yatong Bai, Hyunin Lee, and Somayeh Sojoudi. Initial state interventions for deconfounded imitation learning. In *2023 62nd IEEE Conference on Decision and Control (CDC)*, pages 2312–2319. IEEE, 2023.

Chuan Wen, Jierui Lin, Trevor Darrell, Dinesh Jayaraman, and Yang Gao. Fighting copycat agents in behavioral cloning from observation histories. *Advances in Neural Information Processing Systems*, 33: 2564–2575, 2020.

Jonathan Spencer, Sanjiban Choudhury, Arun Venkatraman, Brian Ziebart, and J Andrew Bagnell. Feedback in imitation learning: The three regimes of covariate shift. *arXiv preprint arXiv:2102.02872*, 2021.

Bernhard Schölkopf, Ralf Herbrich, and Alex J Smola. A generalized representer theorem. In *International conference on computational learning theory*, pages 416–426. Springer, 2001.

Fred M Kusumoto, Mark H Schoenfeld, Coletta Barrett, James R Edgerton, Kenneth A Ellenbogen, Michael R Gold, Nora F Goldschlager, Robert M Hamilton, Jose A Joglar, Robert J Kim, et al. 2018 acc/aha/hrs guideline on the evaluation and management of patients with bradycardia and cardiac conduction delay: executive summary: a report of the american college of cardiology/american heart association task force on clinical practice guidelines, and the heart rhythm society. *Journal of the American College of Cardiology*, 74(7):932–987, 2019.

Yuetian Yu, Ye Gong, Bo Hu, Bin Ouyang, Aijun Pan, Jinglun Liu, Fen Liu, Xiu-Ling Shang, Xiang-Hong Yang, Guowei Tu, et al. Expert consensus on blood pressure management in critically ill patients. *Journal of intensive medicine*, 3(03):185–203, 2023.

Weidong Lan, Bitong He, and Sailing Hu. Admission heart rate and in-hospital mortality in acute myocardial infarction: a contemporary analysis of the mimic-iii cohort. *BMC Cardiovascular Disorders*, 25(1):1–8, 2025.

Appendix for “Causal Imitation Learning Under Measurement Error and Distribution Shift”

A More on Related Work

In this section, we provide a more detailed discussion of related work to complement the concise overview in the main text. We elaborate on prior literature in imitation learning, off-policy evaluation under partial observability, and causal imitation learning.

Imitation Learning. Imitation learning (IL) studies the problem of learning a policy from expert demonstrations (Pomerleau, 1988; LeCun et al., 2006; Russell, 1998; Ho and Ermon, 2016b). Broadly, IL methods can be categorized into *offline*, *online*, and *interactive* approaches. Offline methods such as Behavioral Cloning (BC) (Pomerleau, 1988) learn directly from collected expert trajectories without interaction, while inverse reinforcement learning (Russell, 1998) and adversarial IL methods (Ho and Ermon, 2016b) attempt to infer the expert’s underlying reward or occupancy distribution. Interactive IL algorithms, such as DAgger (Ross et al., 2011) and AggreVaTe (Ross and Bagnell, 2014), extend standard BC by querying an interactive expert to correct errors accumulated during learning. However, such interaction is often infeasible in real-world settings where only a fixed set of demonstrations is available. Our work therefore focuses on the offline setting, but differs from standard IL methods by addressing the presence of unobserved confounders and measurement error in state observations. We aim to recover what the expert *intended* to do in each true state, rather than imitating the corrupted actions observed under noisy measurements.

Off-policy Evaluation in POMDPs. A parallel line of work studies off-policy evaluation in partially observable or confounded environments, typically modeled as Partially Observable Markov Decision Processes (POMDPs) with latent states. Tennenholz et al. (2020) introduce a decoupled POMDP formulation in which an additional observation channel enables recovery of the latent state distribution, allowing unbiased value estimation under strong invertibility assumptions. Miao et al. (2022) study episodic POMDPs under nonparametric models and show that the value of a target policy can be identified using two proxy variables associated with the hidden state through bridge-function-based arguments. Subsequent work extends off-policy evaluation to more general confounded POMDPs and Markov Decision Processes, including minimax-based value estimation (Shi et al., 2022), front-door identification and confidence interval construction (Shi et al., 2024), proximal learning for partially observed systems (Bennett and Kallus, 2024b), and model-based approaches that deconfound both rewards and transitions (Hong et al., 2024). Across these settings, the primary goal is to estimate or evaluate policy values using reward signals, and confounding is modeled as contemporaneous, with latent variables affecting actions and rewards at the same time step. In contrast, our work focuses on imitation learning without rewards, where actions have delayed effects on latent variables and proxy information arises from measurement error in state observations. This leads to a different causal structure and shifts the focus from value estimation to recovering the expert policy.

Imitation Learning with Latent Confounding. Recent work has increasingly framed imitation learning as a causal inference problem, emphasizing that expert demonstrations may be biased by hidden variables that jointly influence states and actions. Early studies revealed that such latent factors induce *causal delusion*, where sequence models incorrectly treat their own actions as evidence about unobserved context (Ortega et al., 2021). This insight motivated a line of interventional IL methods (Vuorio et al., 2022; Swamy et al., 2022b), which correct posterior updates by treating past actions as interventions and rely on on-policy expert feedback such as DAgger (Ross et al., 2011).

Orthogonal to these interactive approaches, several works assume that expert demonstrations are corrupted by latent confounders (possibly unknown even to the expert) and formulate imitation learning as an instrumental-variable problem (Swamy et al., 2021; Shao et al., 2025; Zeng et al., 2025). By mitigating confounding, often due to temporally correlated noise, these methods enable recovery of the underlying policy without requiring an interactive expert. Other efforts study theoretical identifiability of value-equivalent imitation policies

using back-door or front-door adjustments on causal graphs (Zhang et al., 2020; Kumor et al., 2021). A complementary literature examines *causal confusion* arising from spurious correlations in the observation space despite the absence of latent variables (De Haan et al., 2019; Pfrommer et al., 2023; Wen et al., 2020; Spencer et al., 2021).

As summarized in Table 1, prior causal IL methods typically rely on graphical adjustment, interactive expert correction, or instrumental-variable formulations designed for short-range confounding. These approaches do not account for measurement error in state observations, which induces a genuinely temporal confounding structure with delayed effects on actions. In contrast, we reinterpret noisy measurements as proxy variables and derive proximal conditional moment restrictions that recover the expert’s causal policy without interventions or valid instruments, enabling fully offline imitation beyond the scope of existing causal IL frameworks.

B A Simple DGP Illustrating π_{opt} vs. Behavioral Cloning

We provide a simple population example showing that π_{BC1} , π_{BC2} , and π_{opt} can disagree even with infinite data. Consider scalar latent context $U_{t-1} \in \mathbb{R}$, observed state $S_t \in \mathbb{R}$, proxy measurement $W_{t-1} \in \mathbb{R}$, and binary actions $\mathcal{A} = \{0, 1\}$. Let

$$\begin{aligned} U_{t-1} &\sim \mathcal{N}(\mu, \sigma_U^2), \\ S_t &= \alpha U_{t-1} + \varepsilon_S, \quad \varepsilon_S \sim \mathcal{N}(0, \sigma_S^2), \\ W_{t-1} &= U_{t-1} + \varepsilon_W, \quad \varepsilon_W \sim \mathcal{N}(0, \sigma_W^2), \end{aligned}$$

with $(\varepsilon_S, \varepsilon_W) \perp\!\!\!\perp U_{t-1}$. The expert uses both the current observed state and the delayed latent context via a threshold rule

$$A_t = \pi_E(S_t, U_{t-1}) = \mathbb{I}\{\beta_S S_t + \beta_U U_{t-1} \geq c\}, \quad (\text{B.1})$$

for fixed coefficients β_S, β_U and threshold c , and assume $\beta_U > 0$.

Causal target π_{opt} . Under the intervention $\text{do}(S_t = s)$, we have $A_t^{(s)} = \mathbb{I}\{\beta_S s + \beta_U U_{t-1} \geq c\}$. Therefore,

$$\mathbb{P}(A_t^{(s)} = 1) = \mathbb{P}\left(U_{t-1} \geq \frac{c - \beta_S s}{\beta_U}\right).$$

Since $\mathcal{A} = \{0, 1\}$, the interventional argmax satisfies $\pi_{\text{opt}}(s) = 1$ iff $\mathbb{P}(A_t^{(s)} = 1) \geq \frac{1}{2}$, i.e., iff the threshold is below the median of U_{t-1} . For a Gaussian, the median equals the mean, so

$$\pi_{\text{opt}}(s) = \mathbb{I}\{\beta_S s + \beta_U \mu \geq c\}. \quad (\text{B.2})$$

BC1 target π_{BC1} . BC1 is defined by $\pi_{\text{BC1}}(s) = 1$ iff $\mathbb{P}(A_t = 1 \mid S_t = s) \geq \frac{1}{2}$. Because (U_{t-1}, S_t) are jointly Gaussian, $U_{t-1} \mid S_t = s$ is Gaussian with mean

$$m_1(s) := \mathbb{E}[U_{t-1} \mid S_t = s] = \mu + \frac{\alpha \sigma_U^2}{\alpha^2 \sigma_U^2 + \sigma_S^2} (s - \alpha \mu). \quad (\text{B.3})$$

Moreover,

$$\begin{aligned} \mathbb{P}(A_t = 1 \mid S_t = s) &= \mathbb{P}(\beta_S s + \beta_U U_{t-1} \geq c \mid S_t = s) \geq \frac{1}{2} \\ &\iff \beta_S s + \beta_U m_1(s) \geq c, \end{aligned}$$

so

$$\pi_{\text{BC1}}(s) = \mathbb{I}\{\beta_S s + \beta_U m_1(s) \geq c\}. \quad (\text{B.4})$$

Comparing (B.2) and (B.4), whenever $\alpha \neq 0$ and $\beta_U \neq 0$, the posterior mean $m_1(s)$ depends on s , so the decision boundary of π_{BC1} generally differs from that of π_{opt} .

BC2 target π_{BC2} and sensitivity to measurement mechanism. BC2 conditions on both S_t and the proxy W_{t-1} . Define $V_{t-1} = (S_{t-1}, W_{t-1})$; in this static illustration we focus on the dependence on W_{t-1} and write $\pi_{BC2}(s, w)$. Again by joint Gaussianity, $U_{t-1} \mid (S_t = s, W_{t-1} = w)$ is Gaussian with mean

$$m_2(s, w) := \mathbb{E}[U_{t-1} \mid S_t = s, W_{t-1} = w] = \mu + \Sigma_{U,Y} \Sigma_{Y,Y}^{-1} \left(\begin{bmatrix} s \\ w \end{bmatrix} - \begin{bmatrix} \alpha\mu \\ \mu \end{bmatrix} \right), \quad (\text{B.5})$$

where $Y = (S_t, W_{t-1})$, $\Sigma_{U,Y} = (\alpha\sigma_U^2, \sigma_U^2)$, and

$$\Sigma_{Y,Y} = \begin{bmatrix} \alpha^2\sigma_U^2 + \sigma_S^2 & \alpha\sigma_U^2 \\ \alpha\sigma_U^2 & \sigma_U^2 + \sigma_W^2 \end{bmatrix}.$$

As before, $\pi_{BC2}(s, w) = 1$ iff $\beta_S s + \beta_U m_2(s, w) \geq c$, hence

$$\pi_{BC2}(s, w) = \mathbb{I}\{\beta_S s + \beta_U m_2(s, w) \geq c\}, \quad (\text{B.6})$$

which generally depends on w and therefore cannot coincide with the state-only target $\pi_{\text{opt}}(s)$. Furthermore, the conditional mean $m_2(s, w)$ depends on the measurement noise variance σ_W^2 through $\Sigma_{Y,Y}^{-1}$; thus changes in the measurement mechanism (e.g., different devices across domains, modeled as different σ_W^2) can change π_{BC2} even when the expert rule (B.1) and the causal target (B.2) remain unchanged.

Connection to Proposition 3.4. In the DGP above, when $\alpha \neq 0$ we have $S_t = \alpha U_{t-1} + \varepsilon_S$, so $U_{t-1} \not\perp\!\!\!\perp S_t$ and therefore the sufficient condition for $\pi_{BC1} = \pi_{\text{opt}}$ in Proposition 3.4(1) fails; correspondingly, (B.2) and (B.4) yield different decision boundaries unless $\beta_U = 0$ (a degenerate case where the expert ignores U_{t-1}). Likewise, since $W_{t-1} = U_{t-1} + \varepsilon_W$ carries information about U_{t-1} , we also have $U_{t-1} \not\perp\!\!\!\perp (S_t, W_{t-1})$ for non-degenerate noise, so the sufficient condition for $\pi_{BC2}(s, v) = \pi_{\text{opt}}(s)$ in Proposition 3.4(2) fails as well. This illustrates concretely that observational BC targets coincide with the causal target only in rare settings where conditioning on observed covariates does not change the latent context distribution (or where the expert policy effectively does not depend on the latent context).

C Proofs

C.1 Proof of Proposition 2.2

For an arbitrary deterministic policy $\pi : \mathcal{X} \rightarrow \mathcal{A}$. Since $A_t \in \mathcal{A} = \{1, \dots, K\}$ is categorical and $e(\cdot)$ denotes the one-hot encoding, we have

$$\|e(A_t) - e(\pi(X_t))\|_2^2 = \begin{cases} 0, & A_t = \pi(X_t), \\ 2, & A_t \neq \pi(X_t), \end{cases}$$

because two distinct one-hot vectors in \mathbb{R}^K differ in exactly two coordinates.

Taking expectation under $(X_t, A_t) \sim d_{\pi_E}$ yields

$$\begin{aligned} \mathcal{R}(\pi) &= \mathbb{E}[\|e(A_t) - e(\pi(X_t))\|_2^2] \\ &= 2\mathbb{E}[\mathbf{1}\{A_t \neq \pi(X_t)\}] \\ &= 2\mathbb{P}(A_t \neq \pi(X_t)). \end{aligned}$$

Using the law of total expectation, this can be written as

$$\begin{aligned} \mathcal{R}(\pi) &= 2\mathbb{E}[\mathbb{P}(A_t \neq \pi(X_t) \mid X_t)] \\ &= 2\mathbb{E}[1 - p(A_t = \pi(X_t) \mid X_t)]. \end{aligned}$$

Since the outer expectation is taken with respect to the marginal distribution of X_t , minimizing $\mathcal{R}(\pi)$ over all deterministic policies π is equivalent to minimizing the $1 - p(A_t = \pi(x) \mid X_t = x)$ for almost every $x \in \mathcal{X}$. Equivalently, for almost every x , any risk minimizer π^* must satisfy

$$\pi^*(x) \in \arg \max_{a \in \mathcal{A}} p(A_t = a \mid X_t = x).$$

Therefore, any $\pi^* \in \arg \min_{\pi} \mathcal{R}(\pi)$ coincides almost everywhere with a Bayes classifier that selects an action maximizing the conditional action probability.

C.2 Proof of Proposition 3.1

Fix any $s \in \mathcal{S}$ and $a \in \mathcal{A}$. By definition, the causal imitation target is

$$\pi_{\text{opt}}(s) \in \arg \max_{a \in \mathcal{A}} \mathbb{P}(A_t^{(s)} = a).$$

Under the assumed deterministic expert mechanism $A_t = \pi_E(S_t, U_{t-1})$ and standard consistency and temporal ordering, intervening on S_t at level s leaves the latent variable U_{t-1} unchanged and yields

$$A_t^{(s)} = \pi_E(s, U_{t-1}).$$

Therefore,

$$\mathbb{P}(A_t^{(s)} = a) = \mathbb{P}(\pi_E(s, U_{t-1}) = a),$$

where the probability is taken with respect to the marginal (population) distribution of U_{t-1} . Since \mathcal{A} is finite, the event $\{\pi_E(s, U_{t-1}) = a\}$ is measurable and its probability can be written as an expectation of the corresponding indicator function, namely

$$\mathbb{P}(\pi_E(s, U_{t-1}) = a) = \mathbb{E}[\mathbb{I}\{\pi_E(s, U_{t-1}) = a\}].$$

Substituting this representation into the definition of $\pi_{\text{opt}}(s)$ gives

$$\pi_{\text{opt}}(s) \in \arg \max_{a \in \mathcal{A}} \mathbb{E}[\mathbb{I}\{\pi_E(s, U_{t-1}) = a\}],$$

which proves the claim.

C.3 Proof of Corollary 3.2

By definition,

$$\bar{\pi}_E(a \mid s) = \mathbb{P}(\pi_E(s, U_{t-1}) = a) = \mathbb{E}[\mathbb{I}\{\pi_E(s, U_{t-1}) = a\}].$$

Proposition 3.1 states that

$$\pi_{\text{opt}}(s) \in \arg \max_{a \in \mathcal{A}} \mathbb{E}[\mathbb{I}\{\pi_E(s, U_{t-1}) = a\}],$$

and therefore

$$\pi_{\text{opt}}(s) \in \arg \max_{a \in \mathcal{A}} \bar{\pi}_E(a \mid s).$$

Moreover, for any fixed $a \in \mathcal{A}$,

$$\mathbb{E}[\mathbb{I}\{\pi_E(s, U_{t-1}) \neq a\}] = 1 - \mathbb{E}[\mathbb{I}\{\pi_E(s, U_{t-1}) = a\}] = 1 - \bar{\pi}_E(a \mid s).$$

Since subtracting from a constant does not change the optimizer, minimizing $\mathbb{E}[\mathbb{I}\{\pi_E(s, U_{t-1}) \neq a\}]$ over $a \in \mathcal{A}$ is equivalent to maximizing $\bar{\pi}_E(a \mid s)$. Consequently,

$$\pi_{\text{opt}}(s) \in \arg \min_{a \in \mathcal{A}} \mathbb{E}[\mathbb{I}\{\pi_E(s, U_{t-1}) \neq a\}],$$

which completes the proof.

C.4 Proof of Proposition 3.4

We prove the claim by explicitly characterizing the three policies π_{opt} , π_{BC1} , and π_{BC2} in terms of probabilities of the action-induced latent sets $B_a(s)$. The argument proceeds as follows. First, we show that under a deterministic expert mechanism, each action probability can be rewritten as the probability that the latent variable U_{t-1} falls into the corresponding set $B_a(s)$. Next, we use these identities to express the BC targets and π_{opt} as maximizers of different probability functionals over $a \in \mathcal{A}$. Finally, we verify that under the stated independence conditions, these maximization problems coincide, yielding equality of the induced policies up to arbitrary tie-breaking.

Fix any $s \in \mathcal{S}$. For each $a \in \mathcal{A}$, recall the action-induced latent set

$$B_a(s) := \{u \in \mathcal{U} : \pi_E(s, u) = a\}.$$

Since π_E is deterministic and \mathcal{A} is finite, the collection $\{B_a(s)\}_{a \in \mathcal{A}}$ forms a partition of \mathcal{U} .

We first rewrite action probabilities in terms of the sets $B_a(s)$. Because the expert mechanism is deterministic, for any realization,

$$\mathbf{1}\{A_t = a\} = \mathbf{1}\{\pi_E(S_t, U_{t-1}) = a\}.$$

Conditioning on $S_t = s$ therefore yields

$$[\mathbf{1}\{\pi_E(S_t, U_{t-1}) = a\} \mid S_t = s] = \mathbf{1}\{\pi_E(s, U_{t-1}) = a\} = \mathbf{1}\{U_{t-1} \in B_a(s)\}.$$

Taking conditional expectations gives

$$\begin{aligned} \mathbb{P}(A_t = a \mid S_t = s) &= \mathbb{E}[\mathbf{1}\{A_t = a\} \mid S_t = s] \\ &= \mathbb{E}[\mathbf{1}\{\pi_E(s, U_{t-1}) = a\} \mid S_t = s] \\ &= \mathbb{E}[\mathbf{1}\{U_{t-1} \in B_a(s)\} \mid S_t = s] \\ &= \mathbb{P}(U_{t-1} \in B_a(s) \mid S_t = s). \end{aligned}$$

An identical argument, now conditioning on $(S_t, V_{t-1}) = (s, v)$, yields

$$\begin{aligned} \mathbb{P}(A_t = a \mid S_t = s, V_{t-1} = v) &= \mathbb{E}[\mathbf{1}\{A_t = a\} \mid S_t = s, V_{t-1} = v] \\ &= \mathbb{E}[\mathbf{1}\{\pi_E(s, U_{t-1}) = a\} \mid S_t = s, V_{t-1} = v] \\ &= \mathbb{E}[\mathbf{1}\{U_{t-1} \in B_a(s)\} \mid S_t = s, V_{t-1} = v] \\ &= \mathbb{P}(U_{t-1} \in B_a(s) \mid S_t = s, V_{t-1} = v). \end{aligned}$$

Without conditioning, we similarly have

$$\begin{aligned} \mathbb{P}(\pi_E(s, U_{t-1}) = a) &= \mathbb{E}[\mathbf{1}\{\pi_E(s, U_{t-1}) = a\}] \\ &= \mathbb{E}[\mathbf{1}\{U_{t-1} \in B_a(s)\}] \\ &= \mathbb{P}(U_{t-1} \in B_a(s)). \end{aligned}$$

We now characterize the three policies via maximization over $a \in \mathcal{A}$. By definition, the BC1 target satisfies

$$\pi_{\text{BC1}}(s) \in \arg \max_{a \in \mathcal{A}} \mathbb{P}(A_t = a \mid S_t = s),$$

where $\arg \max$ denotes the (nonempty) set of maximizers and a deterministic policy is obtained by applying an arbitrary tie-breaking rule when this set contains more than one element. Substituting the identity above, we obtain

$$\pi_{\text{BC1}}(s) \in \arg \max_{a \in \mathcal{A}} \mathbb{P}(U_{t-1} \in B_a(s) \mid S_t = s),$$

up to ties. Likewise, by definition of the BC2 target,

$$\pi_{\text{BC2}}(s, v) \in \arg \max_{a \in \mathcal{A}} \mathbb{P}(A_t = a \mid S_t = s, V_{t-1} = v),$$

which is equivalent to

$$\pi_{BC2}(s, v) \in \arg \max_{a \in \mathcal{A}} \mathbb{P}(U_{t-1} \in B_a(s) \mid S_t = s, V_{t-1} = v),$$

again up to arbitrary tie-breaking.

Next, we characterize π_{opt} . Under the intervention $do(S_t = s)$, the latent state U_{t-1} is not affected, and the expert continues to act according to the same deterministic mechanism. Thus,

$$A_t^{(s)} = \pi_E(s, U_{t-1}),$$

and for any $a \in \mathcal{A}$,

$$\mathbb{P}(A_t^{(s)} = a) = \mathbb{P}(\pi_E(s, U_{t-1}) = a) = \mathbb{P}(U_{t-1} \in B_a(s)).$$

By definition,

$$\pi_{opt}(s) \in \arg \max_{a \in \mathcal{A}} \mathbb{P}(A_t^{(s)} = a),$$

which is therefore equivalent to

$$\pi_{opt}(s) \in \arg \max_{a \in \mathcal{A}} \mathbb{P}(U_{t-1} \in B_a(s)),$$

up to ties.

Finally, we verify the sufficient conditions for coincidence. If $U_{t-1} \perp\!\!\!\perp S_t$, then for every $a \in \mathcal{A}$,

$$\mathbb{P}(U_{t-1} \in B_a(s) \mid S_t = s) = \mathbb{P}(U_{t-1} \in B_a(s)),$$

so the objective functions inside the $\arg \max$ definitions of $\pi_{BC1}(s)$ and $\pi_{opt}(s)$ coincide pointwise in a . Hence the sets of maximizers are identical, and after tie-breaking, $\pi_{BC1}(s) = \pi_{opt}(s)$ for all s .

Similarly, if $U_{t-1} \perp\!\!\!\perp (S_t, V_{t-1})$, then for every (s, v) and every $a \in \mathcal{A}$,

$$\mathbb{P}(U_{t-1} \in B_a(s) \mid S_t = s, V_{t-1} = v) = \mathbb{P}(U_{t-1} \in B_a(s)),$$

which implies equality of the corresponding $\arg \max$ sets and thus, up to ties,

$$\pi_{BC2}(s, v) = \pi_{opt}(s) \quad \text{for all } (s, v).$$

This completes the proof.

C.5 Proof of Theorem 4.5

By Assumption 2.1, we can write

$$P_{A|Z,s} = P_{A|U,s} P_{U|Z,s}, \tag{C.1}$$

$$P_{W|Z,s} = P_{W|U} P_{U|Z,s}, \tag{C.2}$$

where $P_{A|U,s} \in \mathbb{R}^{|\mathcal{A}| \times k}$, $P_{W|U} \in \mathbb{R}^{|\mathcal{W}| \times k}$, and $P_{U|Z,s} \in \mathbb{R}^{k \times |\mathcal{Z}|}$.

Next, by Assumption 4.4, there exist coarsenings Z'_t of Z_t and W'_{t-1} of W_{t-1} , both taking values in $\{1, \dots, k\}$, such that the matrix

$$P_{W'|Z',s} \in \mathbb{R}^{k \times k}$$

is square and invertible. Restricting (C.2) to these coarsenings gives

$$P_{W'|Z',s} = P_{W'|U} P_{U|Z',s}. \tag{C.3}$$

Since $P_{W'|Z',s}$ is invertible, it follows that $P_{U|Z',s}$ is also invertible and

$$P_{U|Z',s}^{-1} = P_{W'|Z',s}^{-1} P_{W'|U}. \tag{C.4}$$

Now, restricting (C.1) to the same coarsening Z'_t yields

$$P_{A|Z',s} = P_{A|U,s} P_{U|Z',s}. \quad (\text{C.5})$$

Multiplying both sides of (C.5) on the right by $P_{U|Z',s}^{-1}$ and substituting (C.4), we obtain

$$\begin{aligned} P_{A|U,s} &= P_{A|Z',s} P_{U|Z',s}^{-1} \\ &= P_{A|Z',s} P_{W'|Z',s}^{-1} P_{W'|U}. \end{aligned} \quad (\text{C.6})$$

We now identify the interventional action distribution. By consistency and the definition of the intervention $A_t^{(s)}$,

$$P(A_t^{(s)}) = P_{A|U,s} P_U.$$

Substituting (C.6) into the above expression yields

$$P(A_t^{(s)}) = P_{A|Z',s} P_{W'|Z',s}^{-1} P_{W'|U} P_U.$$

Since $P_{W'} = P_{W'|U} P_U$, we conclude that

$$P(A_t^{(s)}) = P_{A|Z',s} (P_{W'|Z',s})^{-1} P_{W'}.$$

Therefore, the interventional action distribution $P(A_t^{(s)})$ is identified. Consequently,

$$\pi_{\text{opt}}(s) \in \arg \max_{a \in \mathcal{A}} p(A_t^{(s)} = a)$$

is identified for all s (up to ties), completing the proof.

C.6 Proof of Theorem 4.8

Fix any s in the support of S_t and any action $a \in \mathcal{A}$. Suppose that the function $h_a(w, s)$ satisfies the confounding bridge equation (4.1), that is,

$$p(A_t = a \mid S_{t-1} = z, S_t = s) = \int h_a(w, s) p(w \mid S_{t-1} = z, S_t = s) dw$$

for all z in the support of S_{t-1} .

Integrating both sides with respect to the latent variable U_{t-1} , we obtain

$$\int p(A_t = a, U_{t-1} = u \mid S_{t-1}, S_t = s) du = \iint h_a(w, s) p(w, U_{t-1} = u \mid S_{t-1}, S_t = s) dw du.$$

Rewriting both sides using the chain rule yields

$$\begin{aligned} &\int p(A_t = a \mid U_{t-1} = u, S_{t-1}, S_t = s) p(U_{t-1} = u \mid S_{t-1}, S_t = s) du \\ &= \iint h_a(w, s) p(w \mid U_{t-1} = u, S_{t-1}, S_t = s) p(U_{t-1} = u \mid S_{t-1}, S_t = s) dw du. \end{aligned}$$

By Assumption 2.1, conditional on $(U_{t-1}, S_t = s)$, the action A_t is independent of S_{t-1} and the proxy W_{t-1} is independent of S_{t-1} . Therefore, the above equality simplifies to

$$\int p(A_t = a \mid U_{t-1} = u, S_t = s) p(U_{t-1} = u \mid S_{t-1}, S_t = s) du$$

$$= \iint h_a(w, s) p(w \mid U_{t-1} = u) p(U_{t-1} = u \mid S_{t-1}, S_t = s) dw du.$$

Then, Assumption 4.6 implies that

$$p(A_t = a \mid U_{t-1} = u, S_t = s) = \int h_a(w, s) p(w \mid U_{t-1} = u) dw$$

By consistency and latent exchangeability,

$$p(A_t^{(s)} = a) = \int p(A_t = a \mid U_{t-1} = u, S_t = s) p(U_{t-1} = u) du.$$

Substituting the expression above yields

$$\begin{aligned} p(A_t^{(s)} = a) &= \int \left\{ \int h_a(w, s) p(w \mid U_{t-1} = u) dw \right\} p(U_{t-1} = u) du \\ &= \int h_a(w, s) \left\{ \int p(w \mid U_{t-1} = u) p(U_{t-1} = u) du \right\} dw \\ &= \int h_a(w, s) p(w) dw. \end{aligned}$$

Therefore, the interventional action probability $p(A_t^{(s)} = a)$ is identified for all $a \in \mathcal{A}$. Consequently,

$$\pi_{\text{opt}}(s) \in \arg \max_{a \in \mathcal{A}} p(A_t^{(s)} = a)$$

is identified for all s (up to ties). This concludes the proof.

C.7 Proof of Proposition 5.1

We first show that for any function h ,

$$\sup_{q \in \mathcal{Q}} \widehat{\mathbb{E}} \left[q(Z, S) \{Y^{(a)} - h(W, S)\} - q(Z, S)^2 \right] - \lambda_{\mathcal{Q}} \|q\|_{\mathcal{Q}}^2 = \frac{1}{4} \{\xi_N(h)\}^{\top} K_{\mathcal{Q}} \left(\frac{1}{N} K_{\mathcal{Q}} + \lambda_{\mathcal{Q}} I_N \right)^{-1} \{\xi_N(h)\}, \quad (\text{C.7})$$

where

$$\xi_N(h) = \frac{1}{N} (Y_j^{(a)} - h(W_j, S_j))_{j=1}^N.$$

To see this, we note that by the generalized representer theorem (Schölkopf et al., 2001), the solution to the inner maximization problem over $q \in \mathcal{Q}$ admits the finite-dimensional representation

$$q(z, s) = \sum_{j=1}^N \alpha_j K_{\mathcal{Q}}((Z_j, S_j), (z, s)).$$

Hence, the optimization over q reduces to an optimization over the coefficient vector $\alpha = (\alpha_j)_{j=1}^N \in \mathbb{R}^N$.

Note that we can write

$$q(Z_i, S_i) = \sum_{j=1}^N \alpha_j K_{\mathcal{Q}}((Z_j, S_j), (Z_i, S_i)) = (K_{\mathcal{Q}}\alpha)_i.$$

Hence,

$$\sum_{i=1}^N q^2(Z_i, S_i) = \sum_{i=1}^N (K_{\mathcal{Q}}\alpha)_i^2 = \|K_{\mathcal{Q}}\alpha\|_2^2 = \alpha^{\top} K_{\mathcal{Q}}^2 \alpha.$$

Therefore, we have

$$\begin{aligned}\widehat{\mathbb{E}}\left[q(Z, S)\{Y^{(a)} - h(W, S)\}\right] &= \frac{1}{N} \sum_{i=1}^N q(Z_i, S_i) \{Y_i^{(a)} - h(W_i, S_i)\} = \alpha^\top K_{\mathcal{Q}} \{\xi_N(h)\}, \\ \widehat{\mathbb{E}}[q^2(Z, S)] &= \frac{1}{N} \sum_{i=1}^N q^2(Z_i, S_i) = \frac{1}{N} \alpha^\top K_{\mathcal{Q}}^2 \alpha, \\ \|q\|_{\mathcal{Q}}^2 &= \alpha^\top K_{\mathcal{Q}} \alpha.\end{aligned}$$

Combining the above expressions, we obtain

$$\begin{aligned}\widehat{\mathbb{E}}\left[q(Z, S)\{Y^{(a)} - h(W, S)\} - q^2(Z, S)\right] - \lambda_{\mathcal{Q}} \|q\|_{\mathcal{Q}}^2 &= \alpha^\top K_{\mathcal{Q}} \{\xi_N(h)\} - \frac{1}{N} \alpha^\top K_{\mathcal{Q}}^2 \alpha - \lambda_{\mathcal{Q}} \alpha^\top K_{\mathcal{Q}} \alpha \\ &= \alpha^\top K_{\mathcal{Q}} \{\xi_N(h)\} - \alpha^\top \left(\frac{1}{N} K_{\mathcal{Q}}^2 + \lambda_{\mathcal{Q}} K_{\mathcal{Q}}\right) \alpha.\end{aligned}$$

Let

$$A := \frac{1}{N} K_{\mathcal{Q}}^2 + \lambda_{\mathcal{Q}} K_{\mathcal{Q}}, \quad b := K_{\mathcal{Q}} \{\xi_N(h)\}.$$

Then the objective function can be written as

$$L(\alpha) = \alpha^\top b - \alpha^\top A \alpha.$$

We therefore consider the maximization problem

$$\max_{\alpha \in \mathbb{R}^N} \alpha^\top b - \alpha^\top A \alpha.$$

Taking derivatives with respect to α and setting them to zero yields

$$\nabla_{\alpha} L(\alpha) = b - 2A\alpha = 0,$$

which implies

$$A\alpha = \frac{1}{2}b.$$

Therefore, the optimal coefficients are given by

$$\begin{aligned}\alpha^* &= \frac{1}{2} A^{-1} b \\ &= \frac{1}{2} \left(\frac{1}{N} K_{\mathcal{Q}}^2 + \lambda_{\mathcal{Q}} K_{\mathcal{Q}} \right)^{-1} K_{\mathcal{Q}} \{\xi_N(h)\} \\ &= \frac{1}{2} \left(\frac{1}{N} K_{\mathcal{Q}} + \lambda_{\mathcal{Q}} I_N \right)^{-1} \{\xi_N(h)\},\end{aligned}$$

where I_N denotes the $N \times N$ identity matrix.

Consequently, we have

$$\sup_{q \in \mathcal{Q}} \widehat{\mathbb{E}}\left[q(Z, S)\{Y^{(a)} - h(W, S)\} - q(Z, S)^2\right] - \lambda_{\mathcal{Q}} \|q\|_{\mathcal{Q}}^2 = \frac{1}{4} \{\xi_N(h)\}^\top K_{\mathcal{Q}} \left(\frac{1}{N} K_{\mathcal{Q}} + \lambda_{\mathcal{Q}} I_N \right)^{-1} \{\xi_N(h)\}, \quad (\text{C.8})$$

where

$$\xi_N(h) = \frac{1}{N} (Y_j^{(a)} - h(W_j, S_j))_{j=1}^N.$$

Therefore, the outer minimization problem in (5.3) is reduced to

$$\hat{h} = \arg \min_{h \in \mathcal{H}} \{\xi_N(h)\}^\top \Gamma \{\xi_N(h)\} + \lambda_{\mathcal{H}} \|h\|_{\mathcal{H}}^2, \quad (\text{C.9})$$

where

$$\Gamma = \frac{1}{4} K_{\mathcal{Q}} \left(\frac{1}{N} K_{\mathcal{Q}} + \lambda_{\mathcal{Q}} I_N \right)^{-1}.$$

We note that by the generalized representer theorem (Schölkopf et al., 2001), the solution to this minimization problem admits the representation

$$h(w, s) = \sum_{j=1}^N \alpha_j K_{\mathcal{H}}((W_j, S_j), (w, s)).$$

Hence, only the coefficient vector $\alpha = (\alpha_j)_{j=1}^N$ needs to be determined.

Recall that

$$\xi_N(h) = \frac{1}{N} (Y_j^{(a)} - h(W_j, S_j))_{j=1}^N,$$

which can be written in vector form as

$$\xi_N(h) = \frac{1}{N} (y_a - K_{\mathcal{H}}\alpha),$$

where $y_a := (Y_1^{(a)}, \dots, Y_N^{(a)})^{\top}$. Moreover,

$$\|h\|_{\mathcal{H}}^2 = \alpha^{\top} K_{\mathcal{H}} \alpha.$$

Therefore, the outer optimization problem reduces to

$$\min_{h \in \mathcal{H}} \{\xi_N(h)\}^{\top} \Gamma \{\xi_N(h)\} + \lambda_{\mathcal{H}} \|h\|_{\mathcal{H}}^2 = \min_{\alpha \in \mathbb{R}^N} \frac{1}{N^2} \alpha^{\top} K_{\mathcal{H}} \Gamma K_{\mathcal{H}} \alpha - \frac{2}{N^2} y_a^{\top} \Gamma K_{\mathcal{H}} \alpha + \lambda_{\mathcal{H}} \alpha^{\top} K_{\mathcal{H}} \alpha + c, \quad (\text{C.10})$$

where $c = \frac{1}{N^2} y_a^{\top} \Gamma y_a$ is a constant independent of α .

This convex quadratic optimization problem admits the solution

$$\alpha^* = \left(K_{\mathcal{H}} \Gamma K_{\mathcal{H}} + N^2 \lambda_{\mathcal{H}} K_{\mathcal{H}} \right)^{\dagger} K_{\mathcal{H}} \Gamma y_a. \quad (\text{C.11})$$

D Numerical Specification of DGP Used in the Simulation Study

In this subsection, we provide the full numerical specification of the data-generating process used in the simulation studies. The latent state, observed state, measurement variable, and action take values in $\{0, \dots, K_U - 1\}$, $\{0, \dots, K_S - 1\}$, $\{0, \dots, K_W - 1\}$, and $\{0, \dots, K_A - 1\}$, respectively, with $(K_U, K_S, K_W, K_A) = (4, 4, 4, 4)$.

The latent confounder $U_t \in \{0, \dots, K_U - 1\}$ evolves according to

$$\mathbb{P}(U_t = k \mid U_{t-1}, S_{t-1}, A_{t-1}) = \text{softmax}(\boldsymbol{\alpha}_0 + \mathbf{A}_U U_{t-1} + \mathbf{A}_S S_{t-1} + \mathbf{A}_A A_{t-1})_k,$$

where $\boldsymbol{\alpha}_0 = \mathbf{0}$, $\mathbf{A}_U = -0.5 \mathbf{I}_{K_U}$, $\mathbf{A}_S = 0.6 \mathbf{I}_{K_U \times K_S}$, and $\mathbf{A}_A = 0.15 \mathbf{I}_{K_U \times K_A}$.

The observed state $S_t \in \{0, \dots, K_S - 1\}$ is generated as

$$\mathbb{P}(S_t = k \mid U_t, U_{t-1}, S_{t-1}, A_{t-1}) = \text{softmax}(\boldsymbol{\beta}_0 + \mathbf{B}_U U_t + \mathbf{B}_{U-} U_{t-1} + \mathbf{B}_S S_{t-1} + \mathbf{B}_A A_{t-1})_k,$$

with $\boldsymbol{\beta}_0 = \mathbf{0}$, $\mathbf{B}_U = 0.15 \mathbf{I}_{K_S \times K_U}$, $\mathbf{B}_{U-} = 0.1 \mathbf{I}_{K_S \times K_U}$, $\mathbf{B}_S = 0.35 \mathbf{I}_{K_S}$, and $\mathbf{B}_A = 0.15 \mathbf{I}_{K_S \times K_A}$.

The measurement variable $W_t \in \{0, \dots, K_W - 1\}$ is sampled according to

$$\mathbb{P}(W_t = k \mid U_t) = \text{softmax}(\boldsymbol{\omega}_0 + \boldsymbol{\Omega}_U U_t)_k,$$

where $\omega_0 = \mathbf{0}$ and $\Omega_U = 1.5 \mathbf{I}_{K_W \times K_U}$.

The expert policy is deterministic and given by

$$A_t = \pi_E(S_t, U_{t-1}) = \arg \max_{k \in \{0, \dots, K_A - 1\}} \text{softmax} \left(\gamma_0 + \Gamma_S S_t + \Gamma_U U_{t-1} \right)_k,$$

with $\gamma_0 = \mathbf{0}$, $\Gamma_S = 0.15 \mathbf{I}_{K_A \times K_S}$, and $\Gamma_U = 1.5 \mathbf{I}_{K_A \times K_U}$.

E Data Preprocessing Details

Variables Description. We focus on a Vital signs routinely collected ICU measurements that capture cardiovascular, respiratory, and hemodynamic status. The observed state at time t is represented by a vector $S_t = (\text{MAP}_t, \text{HR}_t, \text{DBP}_t, \text{SBP}_t, \text{O2Sat}_t, \text{Resp}_t)$, while lactate, $U_t = (\text{Lactate}_t)$, is treated as a latent state variable. Table 2 summarizes the clinical meaning of the variables used in our analysis.

Table 2: Clinical variables used in the analysis.

| Variable | Description |
|----------|---------------------------------------|
| MAP | Mean arterial pressure (mm Hg) |
| HR | Heart rate (beats per minute) |
| DBP | Diastolic blood pressure (mm Hg) |
| SBP | Systolic blood pressure (mm Hg) |
| O2Sat | Pulse oximetry (%) |
| Resp | Respiration rate (breaths per minute) |
| Lactate | Blood lactate concentration (mg/dL) |

Missing data imputation. We perform imputation at the patient level using ICU time (ICULOS) as the temporal index. Patients for whom respiration rate (Resp) is entirely unobserved throughout the ICU stay are excluded, as no data-driven imputation is possible in such cases. For the remaining patients, missing values in Lactate and vital signs are imputed using B-spline interpolation. Outside the observed time range, forward and backward filling is applied to obtain complete trajectories.

Discretization of state and latent variables. After imputing missing values, all variables are discretized via quantile-based method based on their clinical interpretation (Kusumoto et al., 2019; Yu et al., 2023; Lan et al., 2025). For variables with well-established clinical interpretation and risk stratification, namely mean arterial pressure (MAP), heart rate (HR), and systolic blood pressure (SBP), we adopt a clinically motivated three-level discretization. Specifically, MAP is discretized into low perfusion ($= 0$), normal ($= 1$), and elevated ($= 2$) regimes; HR into bradycardia ($= 0$), normal ($= 1$), and tachycardia ($= 2$); and SBP into hypotension ($= 0$), normotension ($= 1$), and hypertension ($= 2$). These categories correspond to standard clinical thresholds and represent qualitatively distinct physiological states that are known to influence treatment decisions.

For the remaining vital signs—diastolic blood pressure (DBP), oxygen saturation (O2Sat), and respiration rate (Resp)—whose empirical distributions exhibit limited variability and strong concentration around the normal range, we apply a binary discretization based on empirical quantiles. Concretely, each of these variables is discretized into a lower ($= 0$) and higher ($= 1$) category. Finally, Lactate is discretized into two categories representing lower ($= 0$) and higher ($= 1$) severity levels.

Generation of expert actions and proxy measurements. Let $S_t = (S_{t,1}, \dots, S_{t,d})$ denote the discretized observed state at time t , where $d = 6$ corresponds to the selected vital signs. The components of S_t take discrete values, with $S_{t,j} \in \{0, 1, 2\}$ for MAP, HR, and SBP, and $S_{t,j} \in \{0, 1\}$ for DBP, O2Sat, and Resp. Let $U_t \in \{0, 1\}$ denote the discretized latent severity state.

The expert policy is deterministic and depends on the current observed state and the previous latent severity. Specifically, the expert action is given by

$$A_t = \pi_E(S_t, U_{t-1}) = \arg \max_{k \in \{0,1,2\}} \text{softmax} \left(\boldsymbol{\gamma}_0 + \mathbf{\Gamma}_S S_t + \mathbf{\Gamma}_U U_{t-1} \right)_k,$$

where $\boldsymbol{\gamma}_0 = \mathbf{0} \in \mathbb{R}^3$, $\mathbf{\Gamma}_S \in \mathbb{R}^{3 \times d}$, and $\mathbf{\Gamma}_U \in \mathbb{R}^{3 \times 1}$.

We further consider two proxy measurements of the latent state. For each proxy $W_t^{(j)}$, $j = 1, 2$, observations are generated as

$$W_t^{(j)} \sim \text{Categorical} \left(\text{softmax} \left(\boldsymbol{\omega}_0^{(j)} + \mathbf{\Omega}_U^{(j)} U_t \right) \right), \quad W_t^{(j)} \in \{0, 1, 2\},$$

where $\boldsymbol{\omega}_0^{(j)} \in \mathbb{R}^3$ and $\mathbf{\Omega}_U^{(j)} \in \mathbb{R}^{3 \times 1}$.

Next, to evaluate performance of different policies under different types of distributional shift, similar to simulation studies in Section 6, we construct two controlled shift scenarios.

Shift on noisy state observations. We consider a measurement mechanism shift that alters the conditional distribution of the proxy variable W_t given the latent state U_t , while leaving the latent process, observed states, and expert actions unchanged. In the baseline setting, the proxy is generated according to

$$\mathbb{P}(W_t = k \mid U_t) = \text{softmax}(\boldsymbol{\omega}_0 + \mathbf{\Omega}_U U_t)_k.$$

To induce a measurement shift, we modify the proxy mechanism for observations appearing after a fixed cutoff index $t_0 = 4000$, which corresponds to the beginning of the test set. Specifically, for all $t \geq t_0$, the proxy-generating parameters are sign-flipped:

$$\mathbb{P}_{\text{shift}}(W_t = k \mid U_t) = \text{softmax}(-\boldsymbol{\omega}_0 - \mathbf{\Omega}_U U_t)_k.$$

This intervention changes the relationship between W_t and U_t without affecting the expert policy, latent state dynamics, or the observed state variables.

Population shift. We additionally consider a population shift implemented through selective sampling. Specifically, we operate on the test set based on temporal ordering, consisting of observations with index $t \geq t_0 = 4000$. From this pool, we construct the final test set by jointly imposing two clinically motivated criteria: (i) the lactate level lies in the top 10% of its empirical distribution (corresponding to Lactate ≥ 10.442 which is the 90% quantile), and (ii) the patient has remained in the ICU for at least 12 hours. The resulting test set therefore concentrates on a subpopulation of more severely ill, late-stage ICU patients.